TECHNICAL NOTE CG000686 | Rev B

# **Visium HD Spatial Applications Performance**

### Introduction

Visium HD Spatial Gene Expression assays map whole transcriptome mRNA (Visium HD WT Panel Spatial Gene Expression) and poly(A) RNA (Visium HD 3' Spatial Gene Expression) expression from tissue sections at single cell scale. This Technical Note introduces key concepts and considerations specific to this technology and discusses the performance of Visium HD assays in terms of resolution and sensitivity.

### **Key Terminology**

In this Technical Note, performance is compared across different 10x Genomics Visium assays. Table 1 below describes these assays and the abbreviations used in this document.

### **Visium HD Assays**

The Visium HD WT Panel Spatial Gene Expression assay allows for whole transcriptome spatial gene expression discovery in FFPE, FF, or FxF human or mouse tissue (Figure 1). The workflow begins with sectioning tissue onto glass slides, tissue staining, and imaging. Tissues are then destained and decrosslinked. Next, tissues are incubated with either human or mouse probes, which allows the probes to hybridize to target mRNAs. Visium HD Slides are thawed and washed in preparation for the assay. After probe ligation, tissue slides and Visium HD Slides are loaded onto the Visium CytAssist instrument, where they are brought into close proximity with one another. Single-stranded ligation products are released from the tissue and are captured by the spatially barcoded oligonucleotides within the Visium HD Slide Capture Area. After probe capture, the Visium HD Slide is removed from the Visium CytAssist for downstream library preparation. Gene expression libraries are then generated from each Capture Area and sequenced. After sequencing, the Space Ranger pipeline is used for downstream data processing (v3.0 or later).

Assay	Capture Method	CytAssist- enabled?	Compatible Sample Types	Abbreviation
Visium v1 3' Spatial Gene Expression	Poly(A)	No	Fresh Frozen	Visium v1
Visium v2 WT Panel Spatial Gene Expression	Probe- based	Yes	Fresh Frozen, Fixed Frozen, Formalin Fixed & Paraffin Embedded	Visium v2
Visium HD WT Panel Spatial Gene Expression	Probe- based	Yes	Fresh Frozen, Fixed Frozen, Formalin Fixed & Paraffin Embedded	Visium HD WT Panel
Visium HD 3' Spatial Gene Expression	Poly(A)	Yes	Fresh Frozen	Visium HD 3'

Table 1. Summary of assays featured in this Technical Note.



## **Contents**

Visium HD Spatial Applications Performance		
Introduction		
Key Terminology		
Visium HD Assays		
Methods Overview	7	
Biomaterials and Reagents	7	
Visium HD WT Panel	7	
Visium HD 3'	7	
Data Analysis	7	
Resolution	10	
Introduction	10	
Visium HD WT Panel	1	
Visium HD 3'	14	
Assay Sensitivity	17	
Data Considerations	22	
gDNA	22	
Reproducibility	22	
Visium HD Slide	22	
Conclusion	27	
Conclusion	27	
References	27	
Appendix	28	
Workflow Comparisons	28	
Document Revision Summary	29	

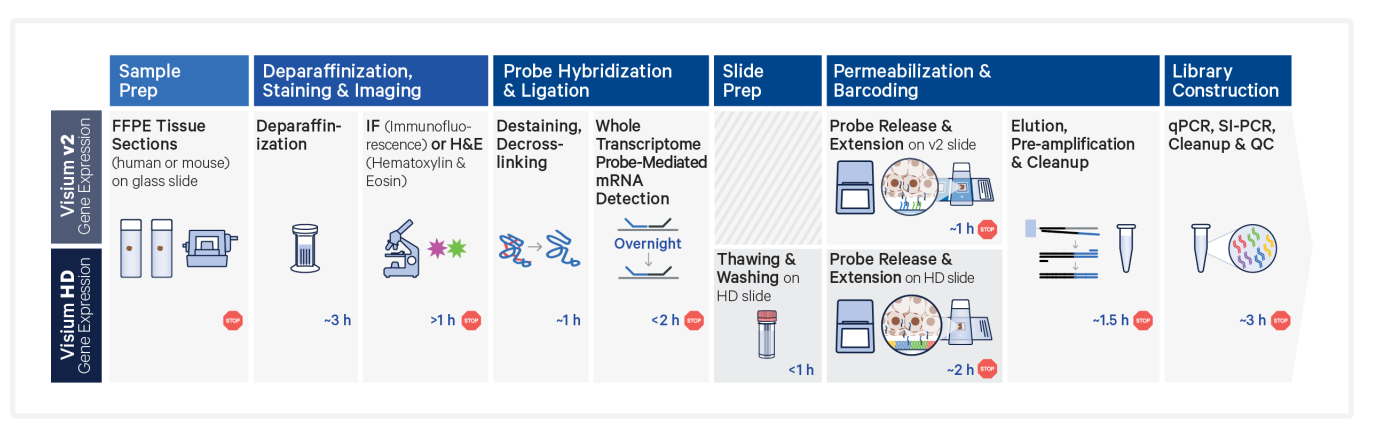


Figure 1. A workflow comparison between Visium HD WT Panel and Visium v2 assays for FFPE tissue. Additional visual overviews for Visium HD WT Panel and Visium v2 for the remaining tissue types can be found in the appendix.



Figure 2. A workflow comparison between Visium HD 3' and Visium v1 assays.

The Visium HD 3' Spatial Gene Expression assay allows for whole transcriptome spatial gene discovery in a variety of species. The workflow begins with sectioning tissue onto glass slides, tissue staining, and imaging (Figure 2). Visium HD Slides are thawed and washed in preparation for the assay. Next, tissue slides are destained and are loaded into the Visium CytAssist instrument along with a Visium HD Slide, where they are brought into proximity with one another. Tissue is permeabilized, allowing for the release of poly(A) RNA and subsequent capture by the spatiallybarcoded oligonucleotides present on the Visium HD Slide surface. The Visium HD Slide is removed from the Visium CytAssist for downstream library preparation. Gene expression libraries are generated from each tissue section and sequenced. Spatial Barcodes are used to associate the reads

back to the tissue section images for spatial mapping of gene expression. After sequencing, the Space Ranger pipeline is used for downstream data processing (v4.0 or later).

The core technology driving Visium HD assays are the barcoded oligonucleotides that link tissue location to gene expression (Figure 2). Visium v2 and Visium v1 slides contain hexagonally arranged barcoded spots that are 55  $\mu m$  in diameter with a distance of 100  $\mu m$  between the center of each spot. By contrast, Visium HD Slides contain 2 x 2  $\mu m$  barcoded squares that are contiguous, forming a continuous lawn of oligos (Figures 3-5).

On the Visium HD Slide, each 2 x 2 µm barcoded square contains a unique Spatial Barcode that allows for mapping gene expression data back to a 10xgenomics.com

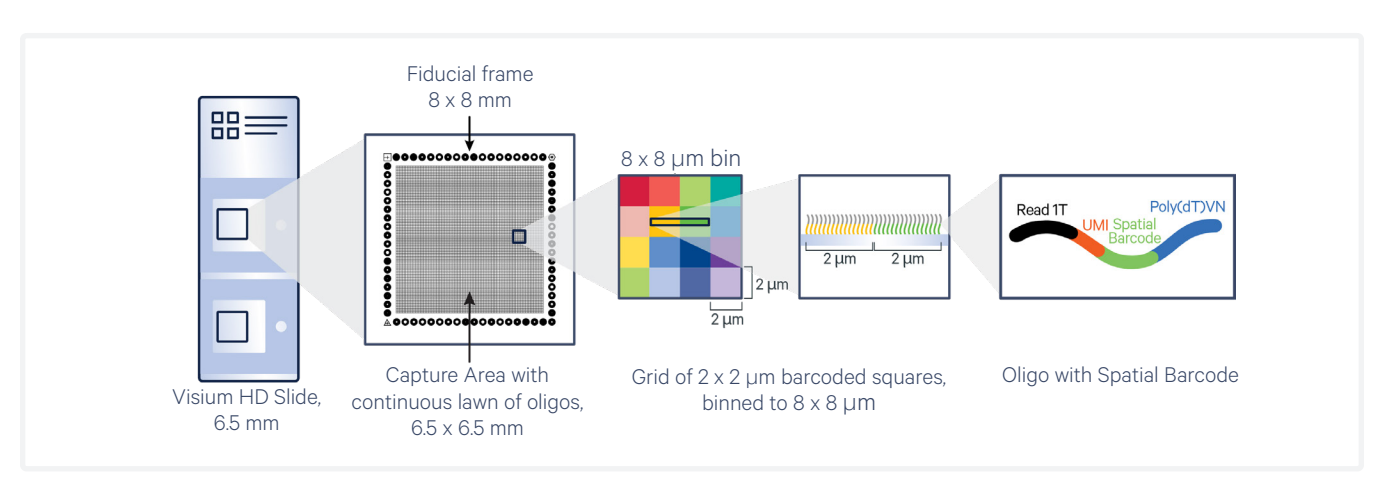
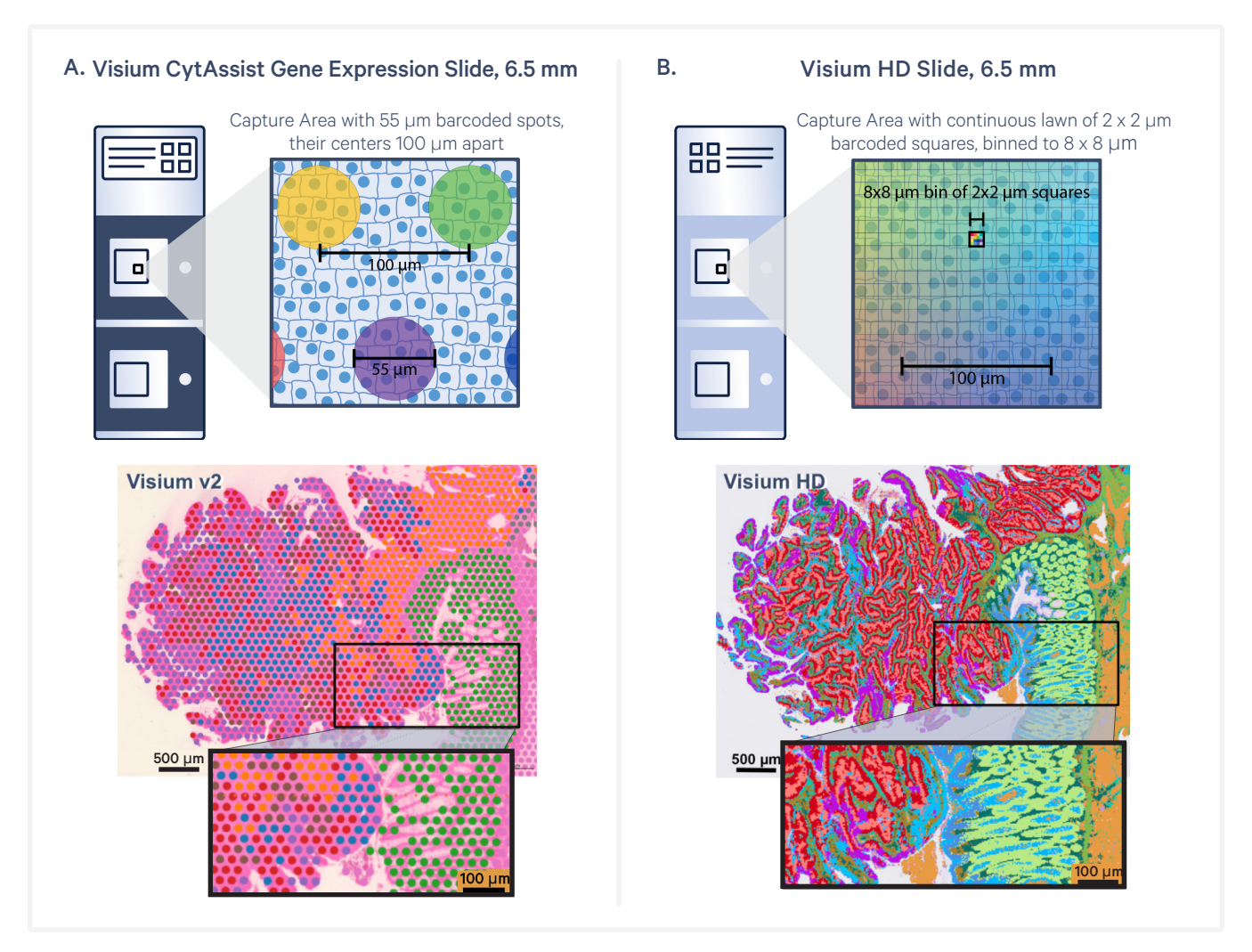
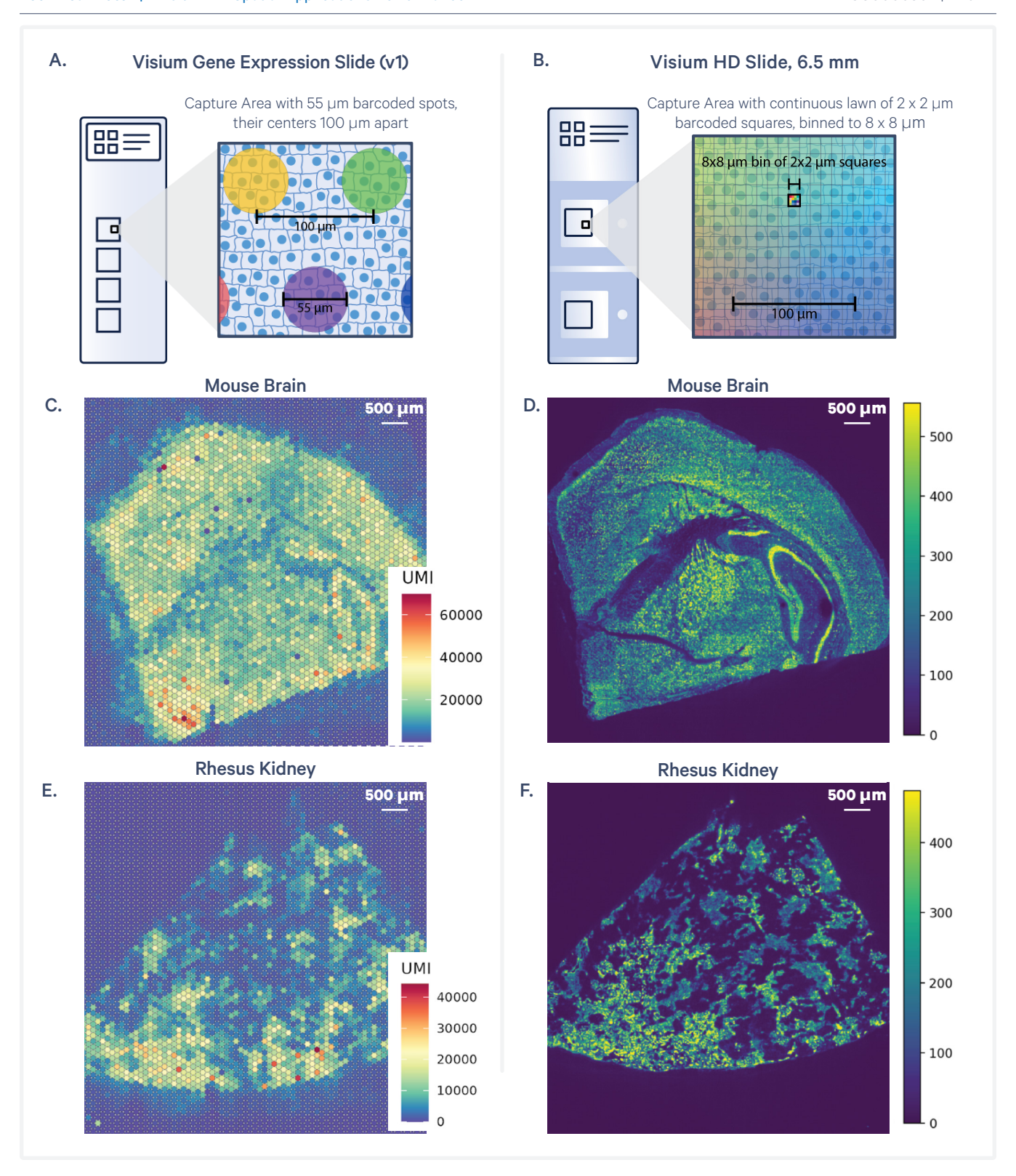


Figure 3. The Visium HD Slide. The Visium HD Slide Capture Area contains spatially barcoded oligos arranged in a grid of  $2 \times 2 \mu m$  barcoded squares.



**Figure 4.** A comparison of sizes between Visium v2 barcoded spots **(A)** and Visium HD barcoded squares for the Visium HD WT Panel assay **(B)**, as well as unbiased clustering for adjacent or near-adjacent human colon cancer sections from the same tissue block. The blue cells shown in the zoomed in view of the Capture Areas are 15 μm wide and are scaled appropriately to the other items within the image.



**Figure 5.** A comparison of sizes between Visium v1 barcoded spots **(A)** and Visium HD barcoded squares for the Visium HD 3' assay **(B)**, as well as unbiased clustering for adjacent or near-adjacent mouse brain **(C-D)** and rhesus kidney **(E-F)** from the same tissue block. The mouse brain had a RIN score of 8.0, while the rhesus kidney had a RIN score of 5.6.

specific square. This lawn of oligos on the Visium HD Slide contains roughly 11 million barcoded squares. Due to the higher number of unique barcodes required, the length of the barcode and UMI region is 43 bases in Visium HD compared to 28 bases for Visium v2 (note that the exact location of individual UMIs and Spatial Barcodes within the 43 base pair region may vary amongst reads). The high-contrast fiducial frame on the Visium HD Slide is imaged by the CytAssist instrument and used downstream by the Space Ranger pipeline to align gene expression data to a microscope image taken of the same tissue section.

The size and continuous nature of the spatially barcoded squares, along with the CytAssist instrument, facilitate mapping gene expression data at single cell scale. The Visium HD Slide and assay are designed to optimize the assay resolution and sensitivity, while enabling alignment of the gene expression data to a high-resolution microscope image of the same tissue section that is taken after staining (Figures 1-2).

# **Methods Overview**

### **Biomaterials and Reagents**

#### Visium HD WT Panel

The following tissue types were used for data generation in this Technical Note:

- Mouse FFPE tissues were obtained in block format from either AcePix Biosciences, BioIVT, or Charles Rivers Labs.
- Human FFPE tissues were obtained in block format from either AcePix Biosciences, Avaden Biosciences, BioIVT, Charles Rivers Labs, Cyence Biopathology, Discovery Life Sciences, or Precision For Medicine.

FFPE tissue blocks were cut into 5  $\mu$ m sections and placed onto Fisherbrand Superfrost Plus slides. Tissue sections were then processed with either the Visium v2 assay or Visium HD WT Panel assay. The probe sets used for each assay are described in Table 2. The Visium HD WT Panel assay uses a new version of the mouse probe set. Samples were prepared using documentation listed in the Appendix.

Species	Assay	Probe Set Version	Kit Part Number	
Mouse	Visium v2	v1	1000365	
	Visium HD WT Panel	v2	1000667	
Human	Visium v2	v2	1000466	
	Visium HD WT Panel	v2		

Table 2. Whole transcriptome probe sets used.

#### Visium HD 3'

The following tissue types were used for data generation in this Technical Note:

- Rodent FF tissues (Mouse, Rat) were obtained snap-frozen from BioIVT or Charles Rivers Labs.
- Human FF tissues were obtained snap-frozen from Avaden Biosciences, BioIVT, Discovery Life

Sciences, or Precision for Medicine.

 Non-rodent vertebrate FF tissues (rhesus monkey, pig, zebrafish) were obtained snap-frozen from AMSBio, Biochemed, and BioIVT.

FF tissue blocks were embedded in OCT, cut into 10 µm sections, and placed onto Visium Slides (Visium v1) or Fisherbrand Superfrost Plus slides (Visium HD for FF and Visium HD 3'). Tissue sections were then processed with either the Visium v1, Visium HD for FF, or Visium HD 3' assays. were prepared using documentation listed in the Appendix.

The Visium HD and HD 3' assays require a Visium CytAssist instrument with firmware 2.0.0 or higher.

### **Data Analysis**

The Space Ranger pipeline was used to process FASTQ files, align reads to probe sets, produce primary output files including the gene-barcode matrices, and generate secondary analysis outputs including unbiased clustering and differential gene expression. Algorithm details can be found in Space Ranger documentation on the 10x Genomics support website. Loupe Browser v8.0 was used for data exploration and visualization of UMI counts, unbiased clustering, and differential gene expression comparisons between clusters. Some input and output files are available on the 10x Genomics public datasets page.

Though each barcoded square is 2 x 2  $\mu$ m, Space Ranger outputs Visium HD data at three bin sizes, offering 8  $\mu$ m and 16  $\mu$ m bin sizes in addition to the native 2  $\mu$ m feature size. Bins offer the advantage of including more mean UMI reads within the bin compared to a 2 x 2  $\mu$ m barcoded square. For example, an 8  $\mu$ m bin provides a 16-fold increase in

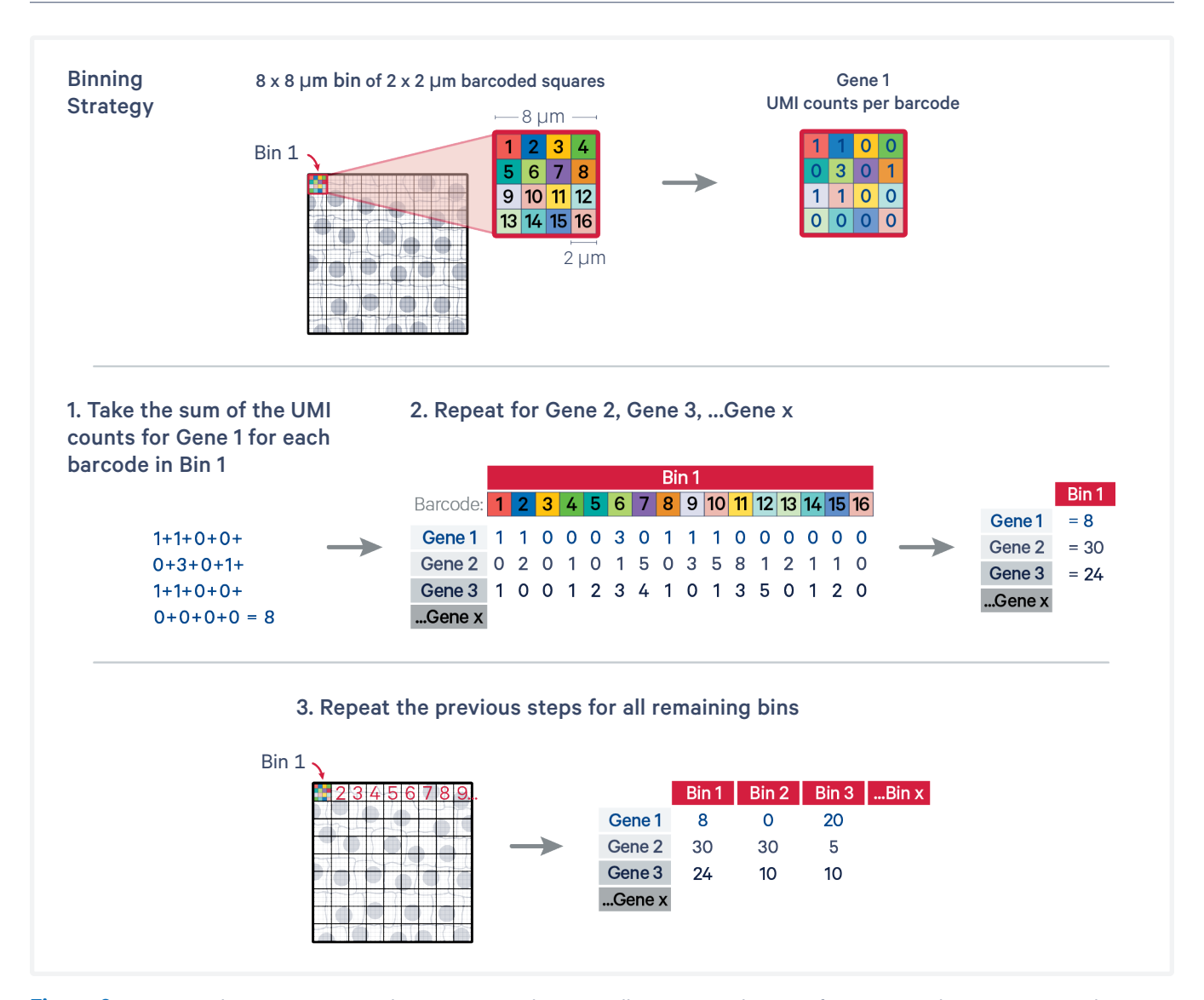


Figure 6. Visium HD binning overview. The UMI counts shown are illustrative and are not from an actual Visium HD sample.

the number of UMI reads on average within the bin compared to a 2  $\mu m$  square. This increase improves the ability to resolve tissue structures via unbiased clustering or other analyses. A custom bin size (in microns at even integer values between 10 and 100) can be defined in Space Ranger or via third-party tools. Although optimal bin size may vary depending on the tissue type or other variables, the 8  $\mu m$  bin size is an effective starting point for most researchers. It is the default binning size used to calculate some of the top-level metrics shown in the web summary and is what is shown in the Loupe Browser visualization. Figure 6 shows an

overview of how Visium HD data are binned. The UMI counts shown in the example are illustrative and are not from an actual Visium HD sample.

In addition to the binning described in the section above, Space Ranger v4.0 enables cell segmentation to be performed on Visium HD WT Panel and Visium HD 3' data with corresponding H&E images (Figure 7). For Space Ranger, cell segmentation refers to the process of identifying and assigning a 2  $\mu$ m bin to a cell ID based on the position of a nucleus, which is used as a starting point to infer the boundary of the cell. To do this, Space Ranger takes a brightfield microscope image of the sample

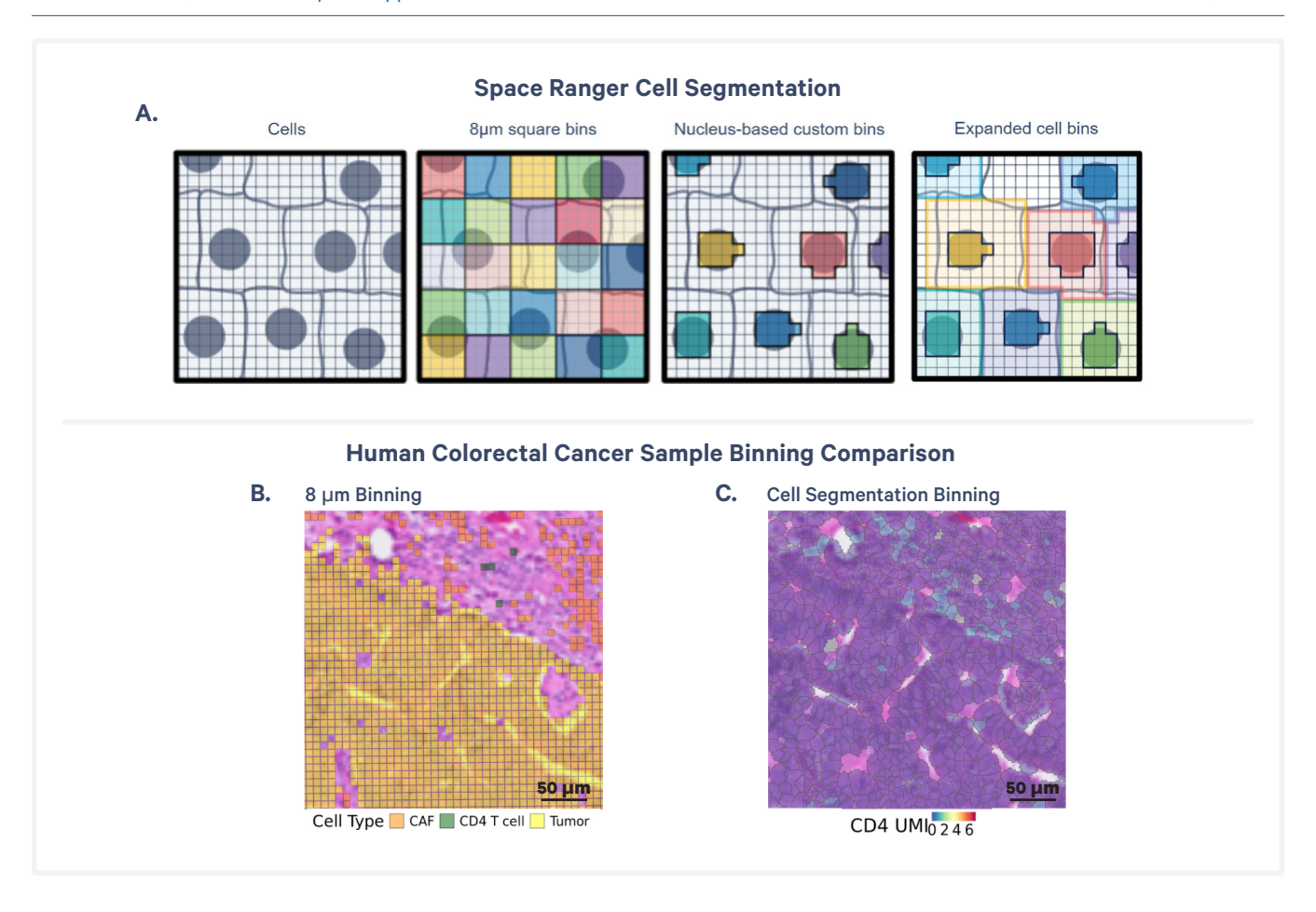


Figure 7. Space Ranger utilizes H&E images to generate expanded cell bins (A). Space Ranger identifies nuclei and assigns each cell ID a 2 μm bin. Based on this bin, the boundary of the cell is inferred. In a human colorectal cancer sample, 8 μm binning (B) reveals some CD4 positive T-cells, while cell segmentation-based binning (C) identifies additional CD4 positive t-cells.

(must be at 20x or greater magnification) and runs a nuclear detection model to each cell nuclei. Next, Space Ranger configures and applies a nuclear expansion mask radiating from the cell nuclei. Lastly, Space Ranger generates segmented genecell matrices and other output files based on these expanded nucleus boundaries.

Space Ranger also supports the use of custom, usersubmitted nuclear segmentation masks generated with third party tools. The model used in this process is a custom implementation of StarDist (Schmidt U, et al. arXIV, 2018), which 10x Genomics trained on >17,000 image patches coming from >150 H&E tissue images from FFPE, fresh frozen, and fixed frozen human and mouse tissues. The use of cell segmentation can help improve spatial resolution, resolving more relevant cell types within identified clusters. To illustrate this, human colorectal cancer samples were used to compare the binned data (8  $\mu$ m bin size) to the segmented data. On the left, the 8  $\mu$ m binning has identified only a small number of CD4+ T cells. On the right, segmentation-based binning has directly identified additional CD4+ T-cells.

Though the model performs well across a variety of tissue types, the accuracy of the model is influenced by the quality of the H&E staining and the density of nuclei. Species with extremely different cellular morphologies from human and mouse (e.g., plants) may have variability in performance.

### Resolution

#### Introduction

Effective spatial resolution is determined by a combination of Spatial Barcode dimensions (i.e., feature size and density), accuracy of transcript localization, and sensitivity. Visium HD assays optimize for these dimensions of spatial resolution through a combination of Capture Area design, the CytAssistenabled assay, and accurate image alignment.

As previously described, the Visium HD Capture Area has a continuous 2 x 2  $\mu$ m lawn of oligos that enable the capture of transcripts at cellular resolution. The 2  $\mu$ m square barcode size is the resolution limit of the assay, but effective spatial resolution also requires minimizing flow and diffusion that

could localize transcripts to the wrong position. To address this, Visium HD assays are performed on the CytAssist instrument, which provides an environment designed to minimize diffusion and flow during target molecule release and capture that would negatively impact accurate transcript localization.

Space Ranger aligns gene expression and imaging information using a three-step process to achieve accurate alignment (Figure 8A). Obtaining gene expression and imaging from the same tissue section versus an adjacent serial section is critical, as tissue section thickness is at the same width of a single cell, resulting in cell composition differences between tissue sections (Figure 8B-C).

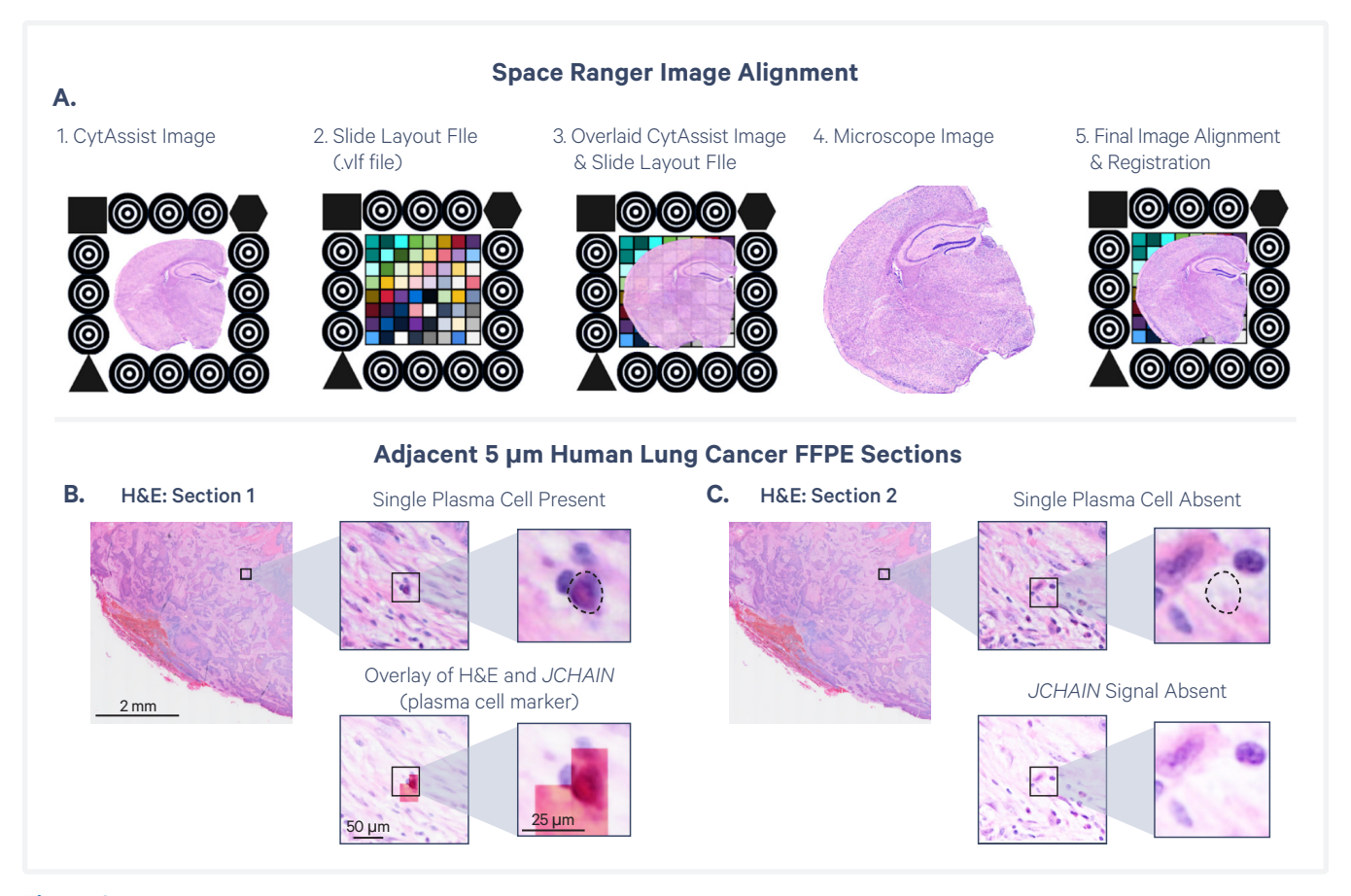
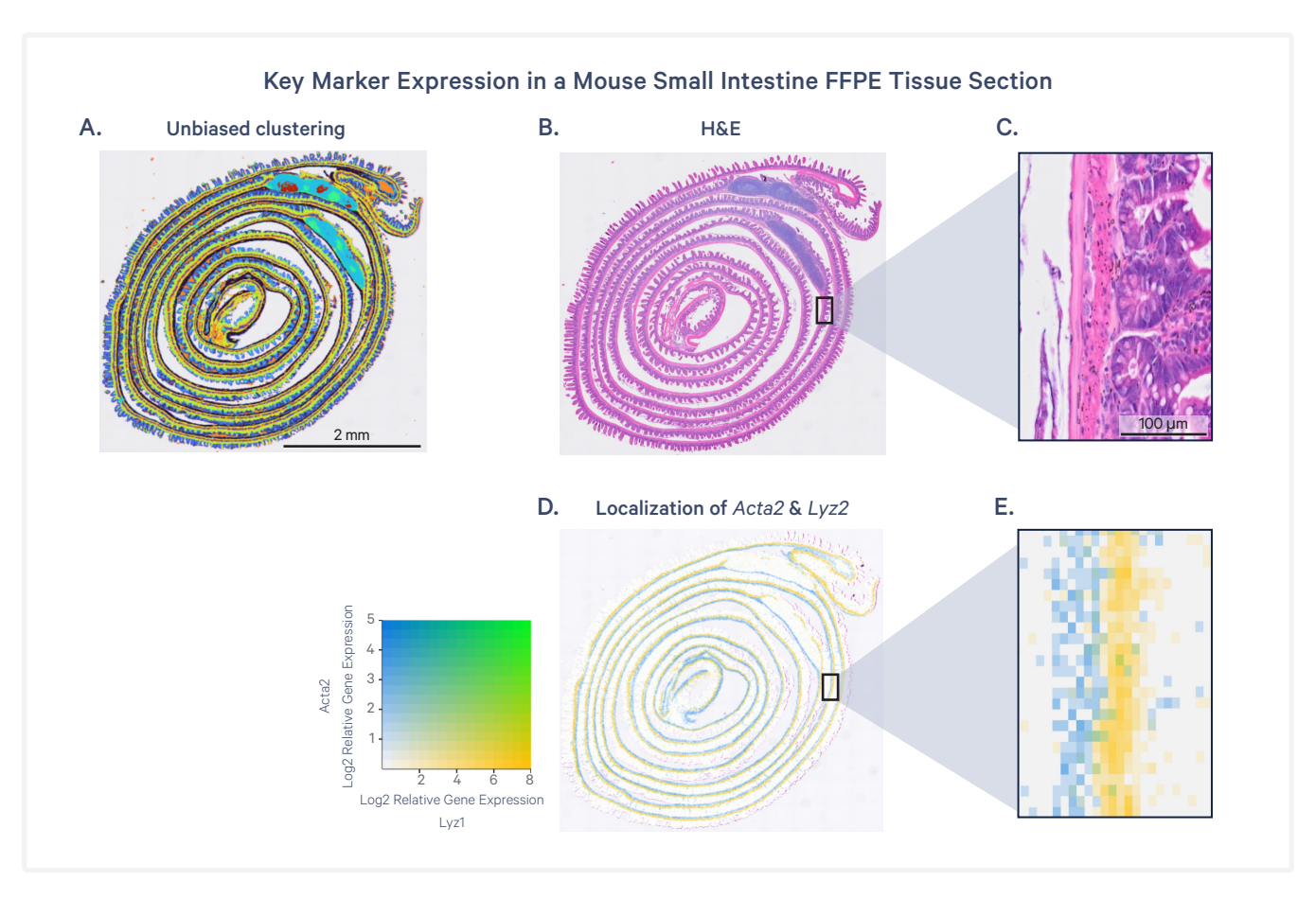


Figure 8. Space Ranger process to achieve accurate alignment between images and gene expression data (A). First, the high-contrast circular fiducials surrounding the Capture Area in the CytAssist image are detected. Then, the slide-specific layout file (vlf file) is used to determine the position and orientation of the barcoded squares relative to the fiducial frame. Finally, Space Ranger aligns the tissue in the CytAssist image to the tissue in the microscope image. By combining these steps, the barcoded squares can be localized both in the CytAssist and microscope images. The fiducial frame in this image is illustrative and is not to scale. In serial human lung cancer samples run simultaneously through the Visium HD assay, a plasma cell is present as marked by JCHAIN in one section (B) and absent in the adjacent section (C).



**Figure 9.** A mouse small intestine FFPE tissue section. Unbiased clustering **(A)** and H&E image **(B)** of the tissue section. A zoomed-in view of the region noted in the black box shows distinct crypts comprised of Paneth cells (dark purple) underlying smooth muscle **(C)**. As expected, the relative gene expression of Paneth cell marker *Lyz1* and the smooth muscle marker *Acta2* appear in distinct layers that correspond to the H&E image **(D-E)**. Colors in D-E correspond to relative gene expression of *Lyz1* and *Acta2* as shown in the heat map.

#### **Visium HD WT Panel**

To demonstrate the accuracy of transcript localization in Visium HD WT Panel data, qualitative and quantitative assessments were performed on mouse intestine FFPE sections based on marker gene expression. The mouse intestine has a known set of unique marker genes specific to adjacent cell types and a repetitive structure (Figure 9). When looking at the gene expression distribution of key markers in Figure 9, the gene expression pattern reveals clearly-defined separation between Paneth cells and underlying smooth muscle cells. Figure 10 shows that within manually annotated regions, 91% of Paneth cell markers are found in Paneth cells, while 86% of smooth muscle markers are found in smooth

muscle. Taken together, these qualitative and quantitative assessments confirm that the Visium HD assay enables accurate transcript localization.

To further illustrate the ability of the Visium HD WT Panel assay to achieve accurate transcript localization, mouse kidney FFPE tissue sections were analyzed (Figure 11). Structurally, the mouse kidney can be divided into three different regions enclosed by a fibrous outer layer called the renal capsule, the cortex, the outer medulla, and the inner medulla. As with the mouse intestine example, the expression of key marker genes shows clearly defined regions of the kidney, with defined borders between each respective layer and very little blurring, even between adjacent cells.

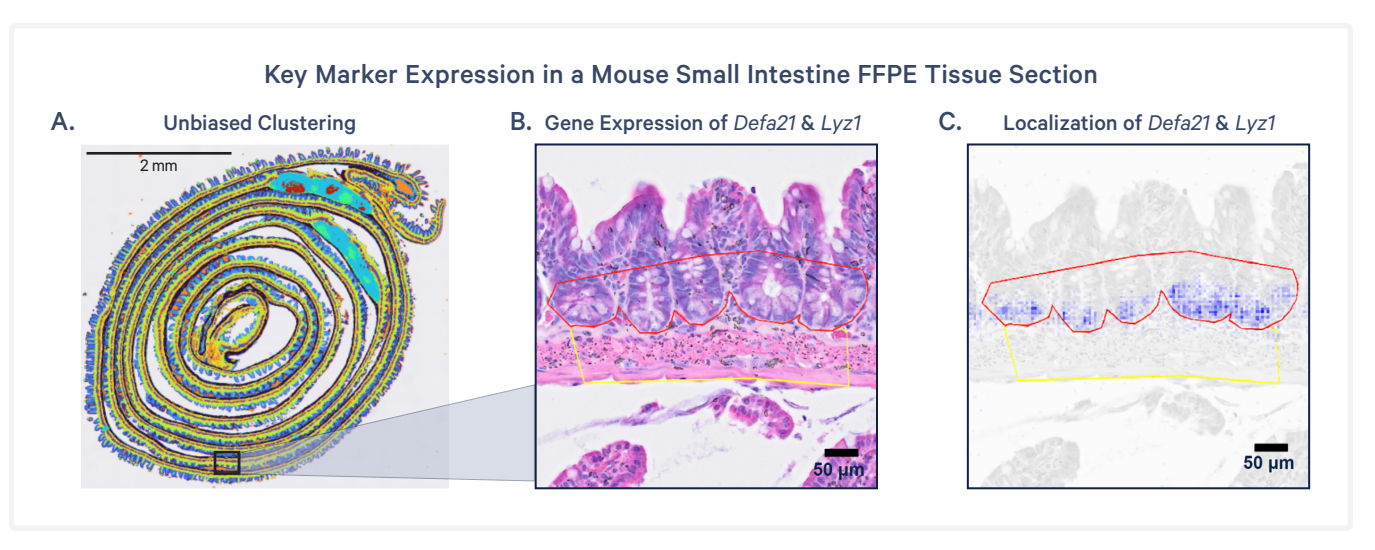


Figure 10. A mouse small intestine FFPE tissue section. (A), H&E image of region marked in the black box (B), and expression of the genes Defa21 and Lyz1 in the same region (C). The red outline is a manual annotation of intestinal crypts, while the yellow outline is a manual annotation of the underlying smooth muscle. In this image, 91% of all Lyz1 and Defa21 expression exists within the red annotated region. When looking at five regions of interest, the fraction of Defa21 and Lyz1 transcripts localized to the appropriate crypt region was 86%, indicating that expected localization remained consistent throughout the tissue.

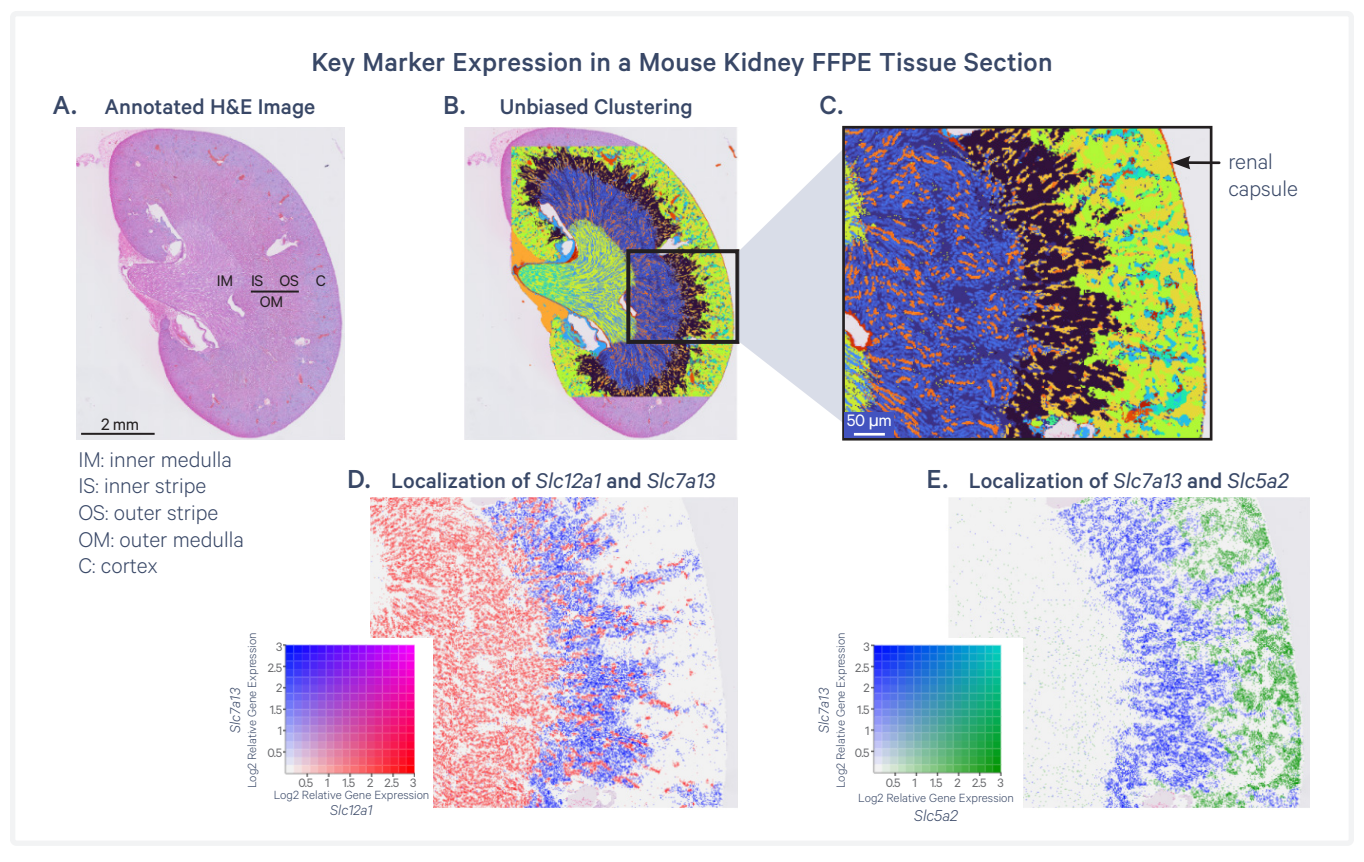


Figure 11. A mouse kidney FFPE tissue section processed with the Visium HD WT Panel assay reveals expected localization of key cell markers. The mouse kidney is divided into three different regions enclosed by a layer called the renal capsule: the cortex (a peripheral layer), the outer medulla (composed of the outer and inner stripes), and the inner medulla as annotated in the H&E image (A). Defined tissue structures matching known kidney regions are revealed by unbiased clustering (B-C). Known gene markers were used to visualize the spatial localization of two regions: Slc12a1, which is expressed by the thick ascending limb of the inner stripe of the outer medulla and Slc5a2, which is expressed by proximal tubules within the outer stripe of the outer medulla (D-E). Colors in D-E correspond to relative gene expression of Slc7a13, Slc12a1, and Slc5a2 as shown in the heat maps.

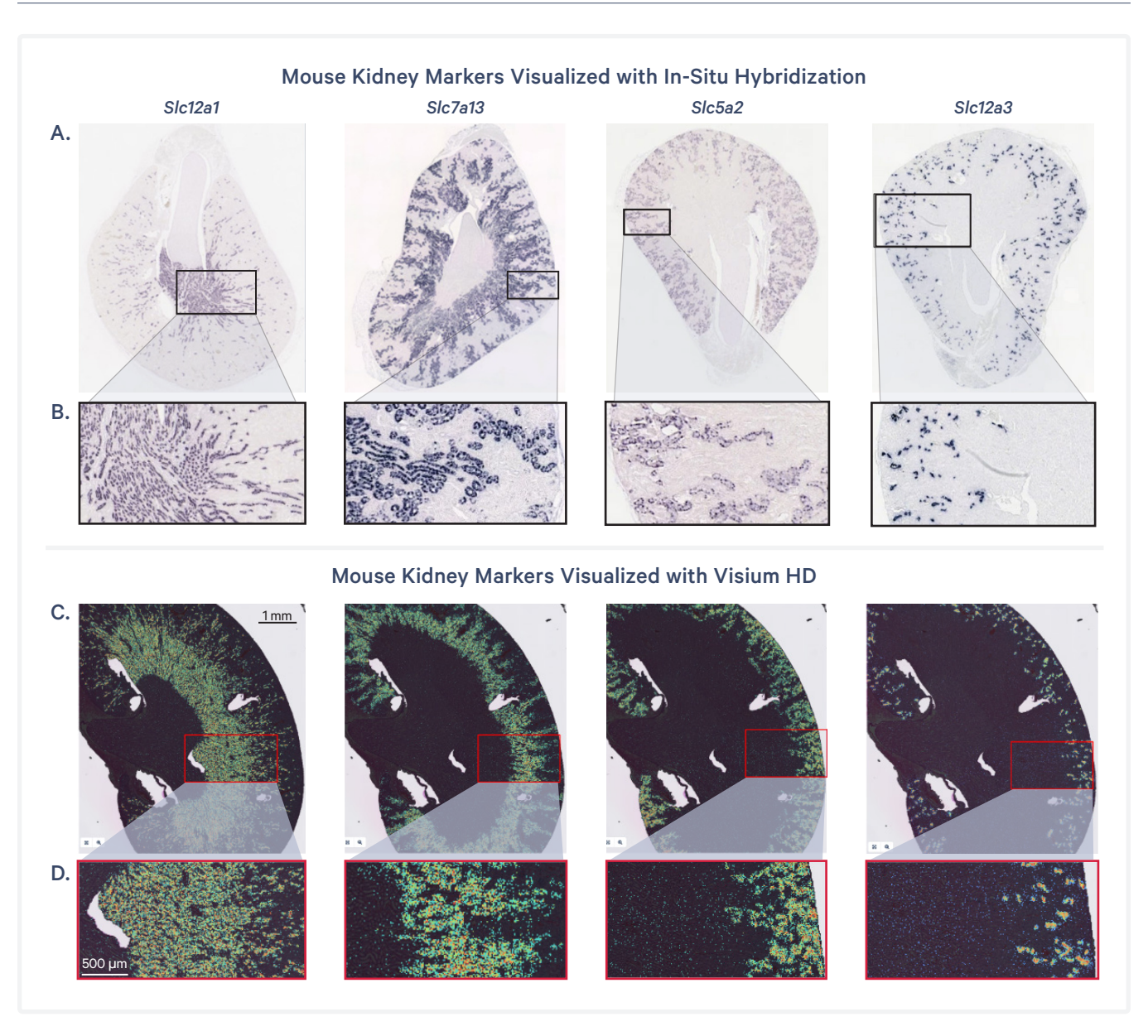


Figure 12. Comparison of Visium HD WT Panel data with publicly available data for mouse kidney FFPE tissue. The spatial expression pattern of Slc12a1, Slc7a13, Slc5a2, and Slc12a3 using in-situ hybridization (Mouse Genome Informatics, The Jackson Laboratories) (A-B) and gene expression from Visium HD using Loupe Browser (C-D) are comparably localized within the mouse kidney.

To confirm that the gene expression patterns detected by the assay match expected patterns based on publicly available data, Visium HD WT Panel data from the mouse kidney was compared to a collection of in-situ hybridization images from

the Jackson Laboratories Mouse Genome Informatics database (Figure 12). As expected, the expression of these key markers in the Visium HD WT Panel data closely matches the in-situ hybridization results.

#### Visium HD 3<sup>1</sup>

To demonstrate the accuracy of transcript localization in Visium HD 3' data, three model systems were chosen: human skin (primary dermal melanoma), mouse eye, and a human/mouse xenograft (human colorectal carcinoma grown in a NSG mouse pup (P1)).

In the skin, the stratum basale is the deepest layer of the epidermis, acting as the primary site of cell division and renewal. It contains keratinocyte stem cells that continuously divide, producing new keratinocytes that are then pushed upwards through the epidermal layers. Directly above the stratum basale lies the stratum granulosum, where keratinocytes begin to flatten and accumulate keratohyalin

granules and lamellar bodies. As keritinocytes continue to move through the stratum granulosum, they undergo programmed cell death and eventually form a layer called the stratum corneum.

Figure 13 shows that all of these layers can be resolved using Visium HD 3'. As shown by key marker expression, the stratum basale forms a distinct layer at the bottom of the epidermis. Markers for the stratum granulosum appear distributed between the stratum basale and stratum granulosum. Additionally, markers for the stratum corneum begin to appear in the stratum granulosum

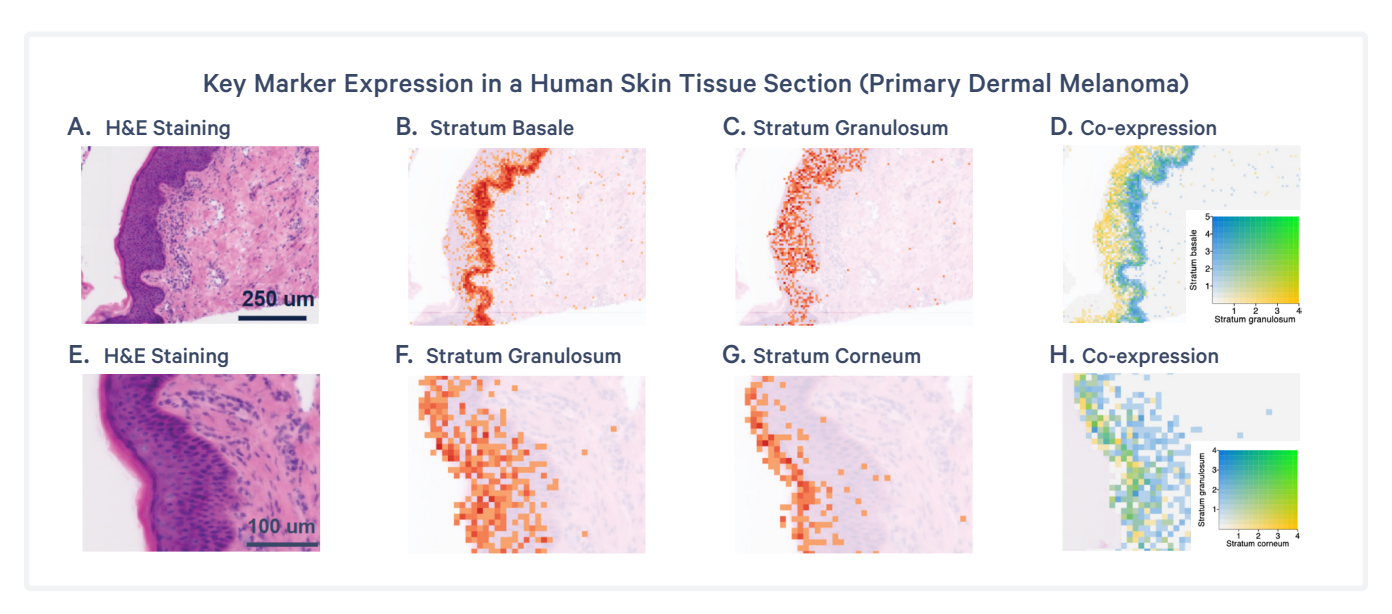


Figure 13. Distinct layers of human skin are resolved by Visium HD 3', with H&E staining shown in (A). The stratum basale (B) is defined by the expression of COL17A, CDH3, EGFR, KRT5, KRT14, KRT15, TP63, and TYRP1. The stratum granulosum (C,F) is defined by the expression of CSTA, DSC1, DSC1, IVL, SLPI, SBSN, and TGM1. The stratum corneum is defined by the expression of SPINK5, CASP14, KLK5, KLK7, FLG, and LORICRIN (G). Co-expression of stratum basale and stratum granulosum genes are shown in (D) and co-expression of stratum granulosum and stratum corneum genes are shown in (H). Data are binned at 8 µm.

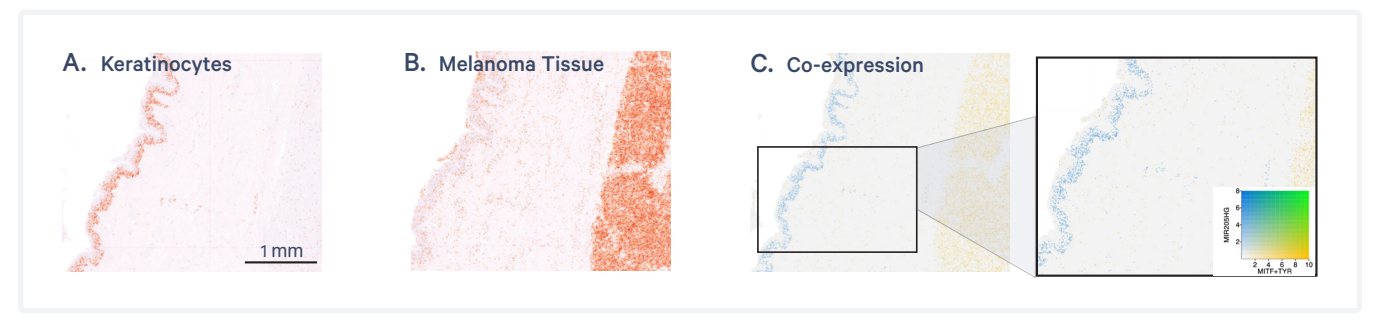


Figure 14. Expression of MIR205HG in human keratinocytes, as well as MITF and TYR in melanoma cells. Data are binned at 8 µm.

but are more highly enriched at the top most layer, suggesting that these dead cell are accumulating at the stratum corneum.

The Visium HD 3' assay captures poly(A) target molecules. Figure 14 shows the detection of MIR205HG, a long non-coding RNA that hosts the microRNA miR-205 within its intronic region. This microRNA is important in maintaining skin homeostasis and its disregulation can contribute to disease. As expected, MIR205hg is shown to be highly expressed in basal keratinocytes. Additionally, the melanoma markers MITF and TYR are highly expressed in a distinct layer under the dermis.

The eye is a highly structured organ. It has numerous cell types organized into distinct layers and structures that carry out various tasks critical to detecting light. In the mouse eye sample in Figure 15, an array of key marker genes are used to resolve structures in the eye. A full list of markers used is in the figure legend.

The cornea, which focuses light as it enters the eye, has specific expression of KRT12. The resulting protein, KRT12, is important for the structure and function of the corneal epithelium. Behind the cornea is the iris, a muscular diaphragm that controls the size of the pupil. The iris shows expression of TYR, important for the melanin production that gives the iris its color. Behind the cornea is the lens, which helps further focus light onto the retina. MIP shows specific expression in the lens and is important for maintaining lens transparency.

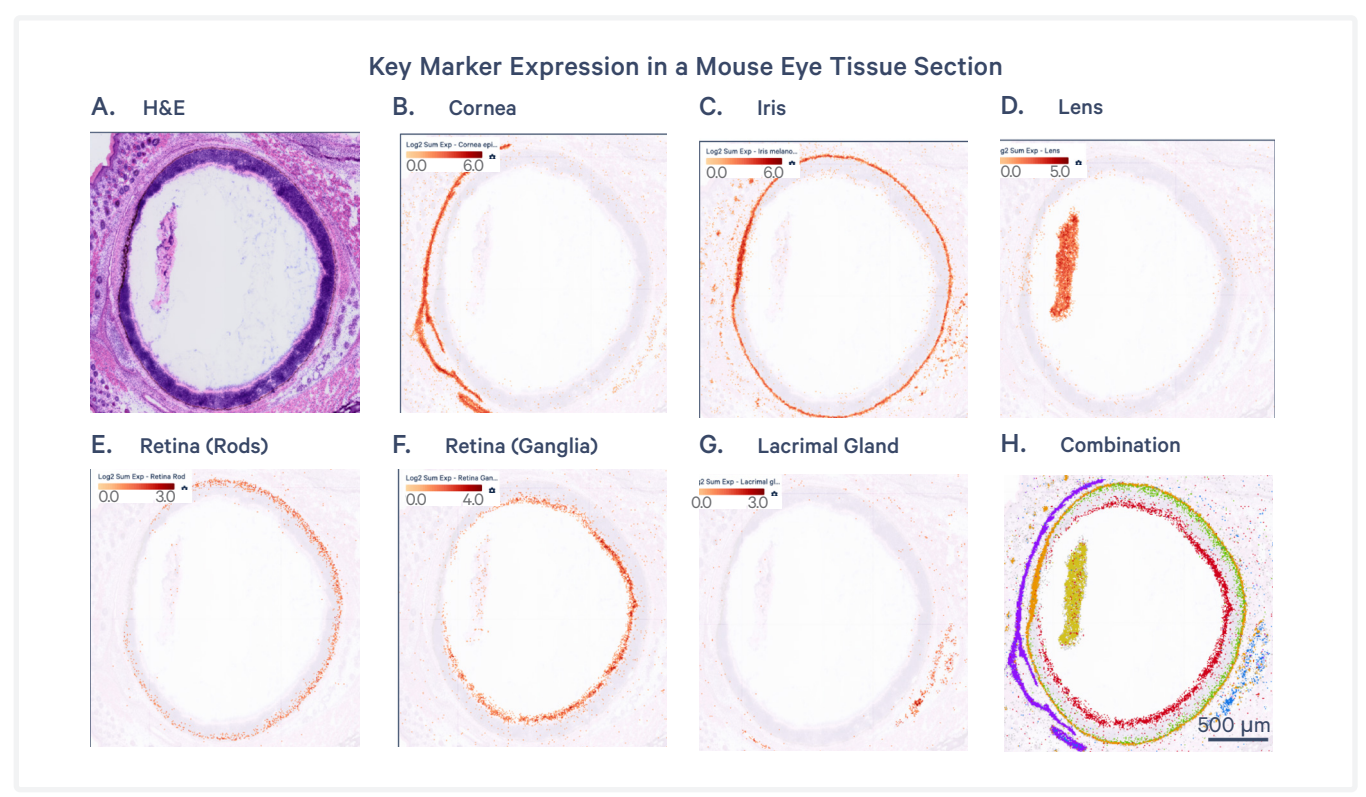


Figure 15. A mouse eye tissue section processed with the Visium HD 3' assay reveals distinct functional layers of the eye. H&E image (A). Defined tissue structures matching known sections of the eye are revealed by the expression of the following genes. Cornea: GPHA2, COL17A1, KRT12, KRT15 (B). Iris: DCT, TYR, TYRP1, PMEL (C). Lens: BFSP2, MIP (D). Retina (rods): RHO, NR2E3 (E). Retina (ganglia): CALB2, IGFBPL1, SNCG, POU4F2, SLC17A6 (F). Lacrimal gland: SOX10, AQP5, LTF (G). A combination of all markers (H). The scale bar in (H) applies to all panels. Data are binned at 8 µm.

In the back of the eye, photoreceptor cells called rods detect light and are characterized by the expression of RHO, which translates to the lightsensitive protein rhodopsin. Rods transmit signals to neurons called ganglia, whose axons converge to form the optic nerve. SNCG is expressed specifically in this layer of the eye and codes for a member of the synuclein family of proteins. Finally, the lacrimal gland can be identified via the expression of AQP5, which is important for tear generation.

The Visium HD 3' assay does not rely on a single, species-specific probe set. Instead, Visium HD 3' captures polyadenylated RNA released from the tissue. Thus, it is can be an ideal assay for

performing a multi-species experiment. Figure 16 shows an example of a xenograft made with a human colorectal carcinoma cell-derived tumor grown in an NSG mouse.

Expression of makers characterizing mouse dermal fibroblasts shows a distinct band of cells at the surface of the xenograft, separate from the human tumor niche. Within the human tumor itself, marker genes separating the niche from a proangiogenic zone are seen. The pro-angiogenic zone is at the periphery of the tumor niche, favoring the creation of blood vessels that connect the human tissue with the host mouse tissue.

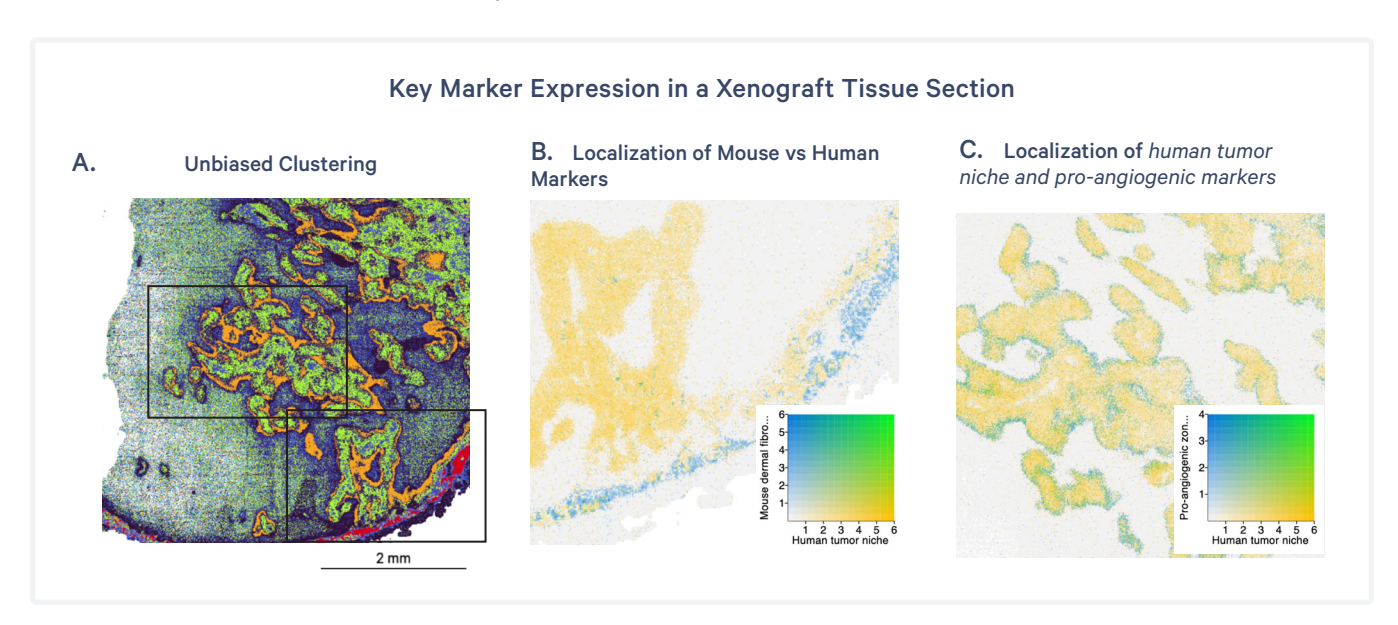


Figure 16. A xenograft section processed with the Visium HD 3' assay reveals distinct regions of a human tumor, as well as clear differentiation between mouse and human tissue. Unbiased clustering (A). Separation between mouse and human tissue are revealed by the expression of the following genes: Mouse (blue): Lum, Dcn, Col1a1, Col3a1, Col5a2, Col6a3, and Col5a1; Human (yellow): LGALS3BP, GES4, GPRC5C, LY6E, ISG15, and IFI27. Within the human tumor, the human tumor niche is distinguished from a layer of pro-angiogenic activity marked by NDRG1 and ANGPTL4 (blue). Data are binned at 8 µm.

### **Assay Sensitivity**

Assay sensitivity refers to the ability of the assay to detect transcripts of interest. To assess sensitivity, defined as the number of unique transcripts detected for Visium HD assays, UMIs are counted on a pertissue area basis. Due to differences in slide design between Visium v2/v1 and Visium HD, making sensitivity comparisons on a per-tissue area is a more biologically relevant comparison than making peractive area (e.g., per-spot or per-square) comparisons. The Visium HD Slide enables target molecule capture under 100% of tissue over the Capture Area. For Visium v1 and Visium v2, a portion of molecules may come from tissue located between barcoded spots (Figures 2-3). Thus, per-area comparisons describe the maximum amount of information that can be obtained from the sample.

Figure 17 compares assay sensitivity between Visium v2 and Visium HD WT Panel across various tissues. For most examples, Visium HD WT Panel sensitivity is ether similar to or exceeds Visium v2 sensitivity at matched sequencing depths. Tissue type, tissue composition, and tissue block quality will impact assay sensitivity. Note that the Visium HD WT Panel assay uses a new version of the mouse probe set, contributing to gains in sensitivity in mouse tissues.

Similarly, Figure 18 compares assay sensitivity between Visium v1 and Visium HD 3' Gene Expression. For most sample types, Visium HD 3' shows sensitivity that is significantly higher than Visium v1 sensitivity at matched sequencing depths. Figure 19 shows that sensitivity is higher for samples processed with Visium HD WT Panel for FF tissues vs. Visium HD 3'. This is most likely attributable to the specificity of the probe-based chemistry. Figure 20 shows that overall gene expression between the two assays shows high correlation and again confirms the higher sensitivity of the Visium HD WT Panel assay.

When evaluating sensitivity in the context of a specific sample, it is important to assess sequencing depth (i.e., the number of total reads per unit tissue area) and sequencing saturation (related to the number of reads sequenced per distinct UMI). In some tissue types, sequencing above the recommended sequencing depth can result in much higher per-bin sensitivity (total UMIs per bin). An example of a human lung cancer sequenced at varying depths and reaching saturation at 6X the recommended sequencing depth is shown in Figure 21. However, there are diminishing returns for additional sequencing for samples with high sequencing saturation. Space Ranger provides web summary that contains a percent sequencing saturation metric together with sensitivity curves. These can be used as a guide to determine the value in deeper sequencing. For more information on making sensitivity comparisons between Visium v2 and Visium HD WT Panel assays, consult the "How do I Compare the Sensitivity of Visium HD to Visium v2" knowledge base article on the 10x Genomics support website.

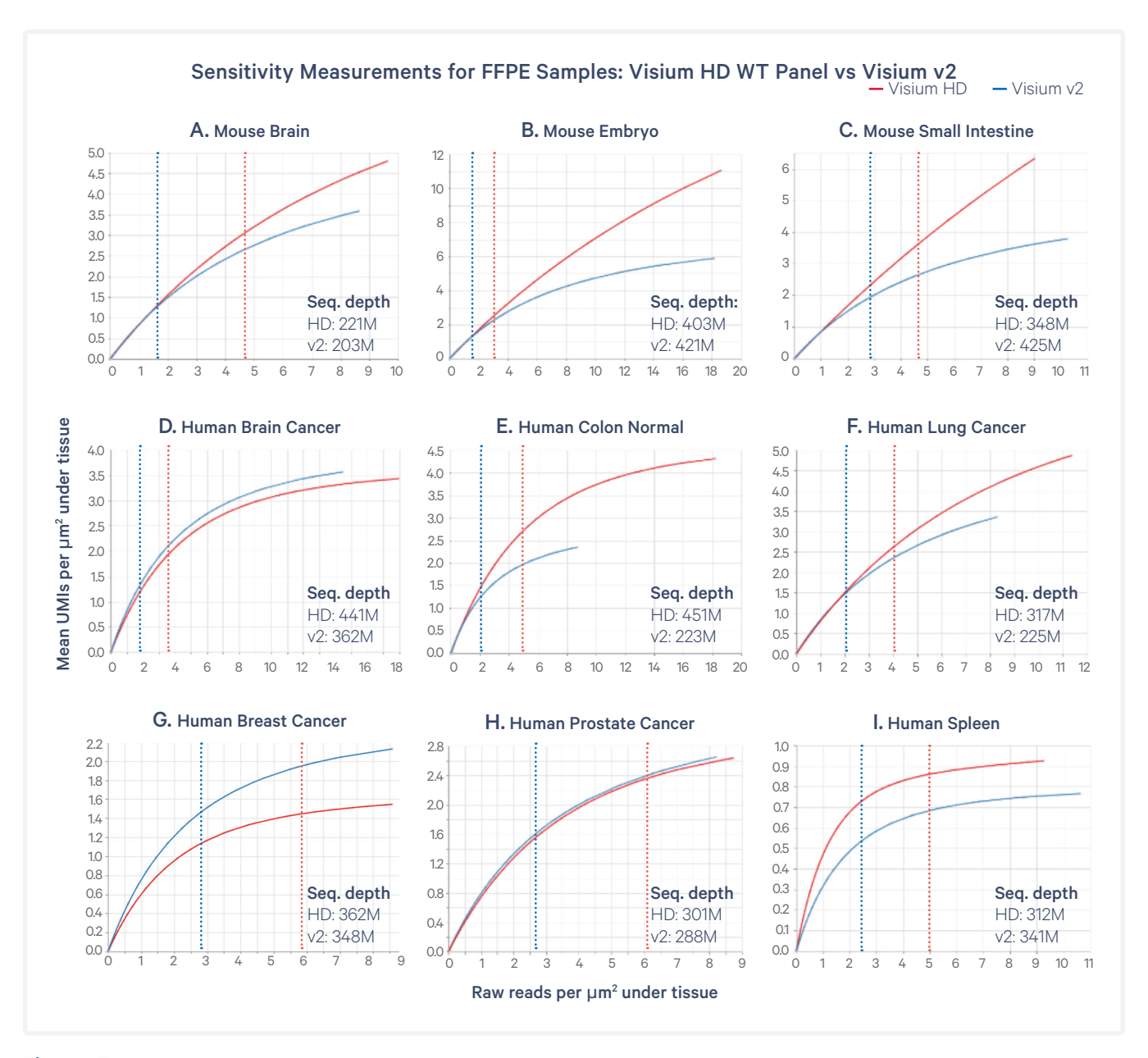


Figure 17. Sensitivity measurements at comparable sequencing depths for the following FFPE samples: mouse brain (A), mouse embryo (B), mouse small intestine (C), human brain cancer (D), human normal colon (E), human lung cancer (F), human breast cancer (G), human prostate cancer (H), and human spleen (I). Sensitivity analysis is averaged across all sections/tissue types. Vertical dotted lines represent the minimum recommended sequencing depth for Visium HD WT Panel (red) and Visium v2 (blue). For FFPE tissue processed with the Visium HD WT Panel assay, this is 275 million reads multiplied by the % Capture Area covered by tissue. For Visium v2, this is % Capture Area covered by tissue multiplied by 5,000 spots multiplied by 25,000 reads/spot. When compared to Visium v2, samples processed with the Visium HD WT Panel assay demonstrate comparable or better performance, though this is largely tissue-dependent. Some tissues, such as human spleen, show sequencing saturation as sequencing depth increases. Other tissues, such as mouse intestine, do not show sequencing saturation as sequencing depth increases. While 10x Genomics provides a recommended sequencing depth, the ideal sequencing depth may be tissue-dependent.

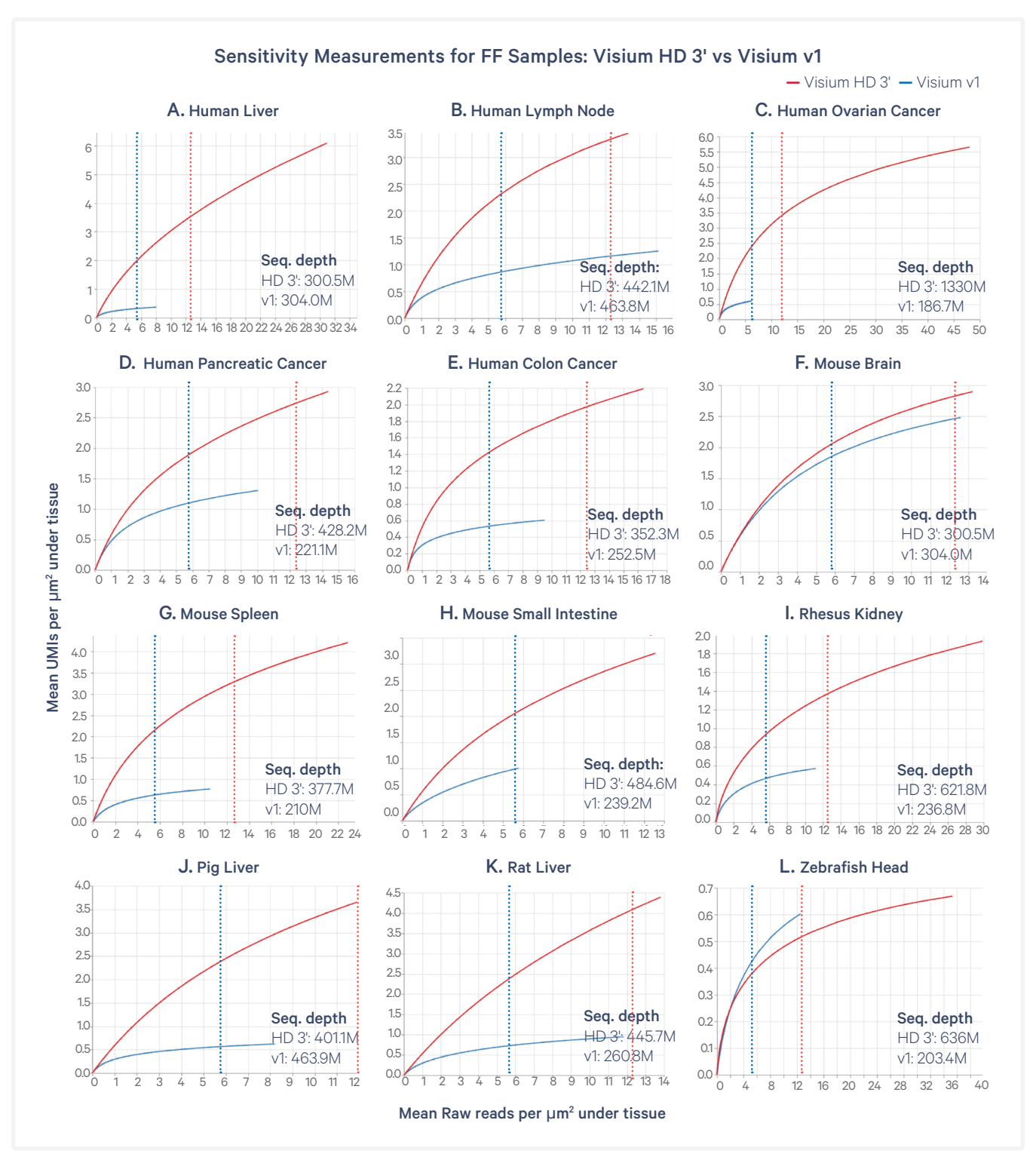


Figure 18. Sensitivity measurements at comparable sequencing depths for the following FF samples: human liver (A), human lymph node (B), human ovarian cancer (C), human pancreatic cancer (D), human colon cancer (E), mouse brain (F), mouse spleen (G), mouse small intestine (H), rhesus kidney (I), pig liver (J), rat liver (K), and zebrafish head (L). Sensitivity analysis is averaged across all sections/tissue types. Vertical dotted lines represent the minimum recommended sequencing depth for Visium HD 3' (red) and Visium v1 (blue). For FF tissue processed with Visium HD 3', this is 550 million reads multiplied by the % Capture Area covered by tissue. For Visium v1, this is % Capture Area covered by tissue multiplied by 5,000 spots multiplied by 50,000 reads/ spot. When compared to Visium v1, samples processed with the Visium HD 3' demonstrate comparable or better performance, though this is largely tissue-dependent. While 10x Genomics provides a recommended sequencing depth, the ideal sequencing depth may be tissue-dependent.

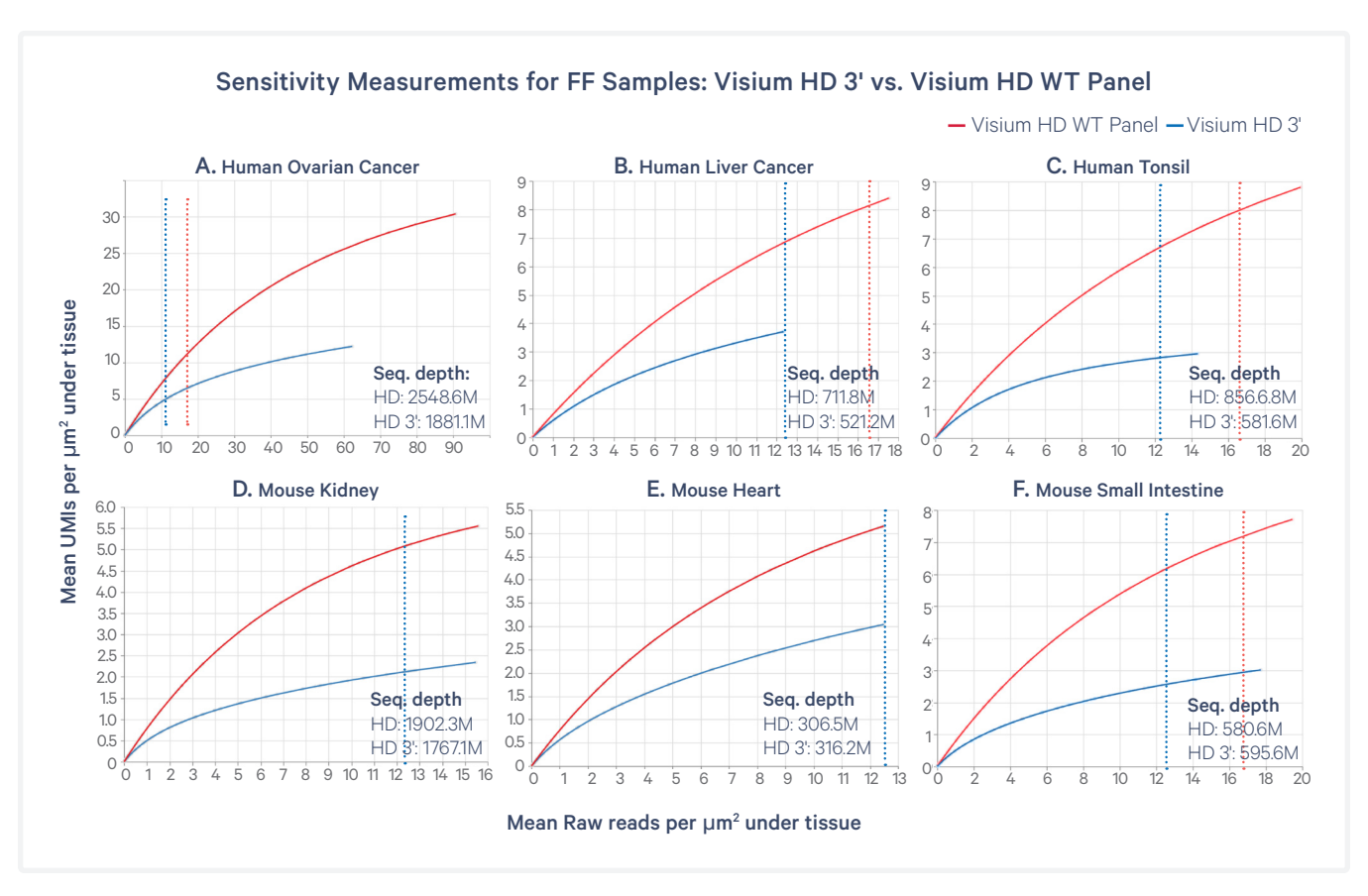


Figure 19. Sensitivity measurements at comparable sequencing depths for the following FF samples: human ovarian cancer (A), human liver cancer (B), human tonsil (C), mouse kidney (D), mouse heart (E), and mouse kidney (F) Sensitivity analysis is averaged across all sections/tissue types. Vertical dotted lines represent the minimum recommended sequencing depth for Visium HD WT Panel (red) and Visium HD 3' (blue). For FF tissue processed with the Visium HD 3' assay, this is 550 million reads multiplied by the % Capture Area covered by tissue. For Visium FF tissue processed with the Visium HD WT Panel assay, this is 275 million reads multiplied by the % Capture Area covered by tissue. When compared to Visium HD 3', samples processed with the Visium HD WT Panel assay demonstrate comparable or better performance. While 10x Genomics provides a recommended sequencing depth, the ideal sequencing depth may be tissue-dependent. For mouse kidney and mouse heart, Visium HD WT Panel samples were not sequenced to the recommended sequencing depth.

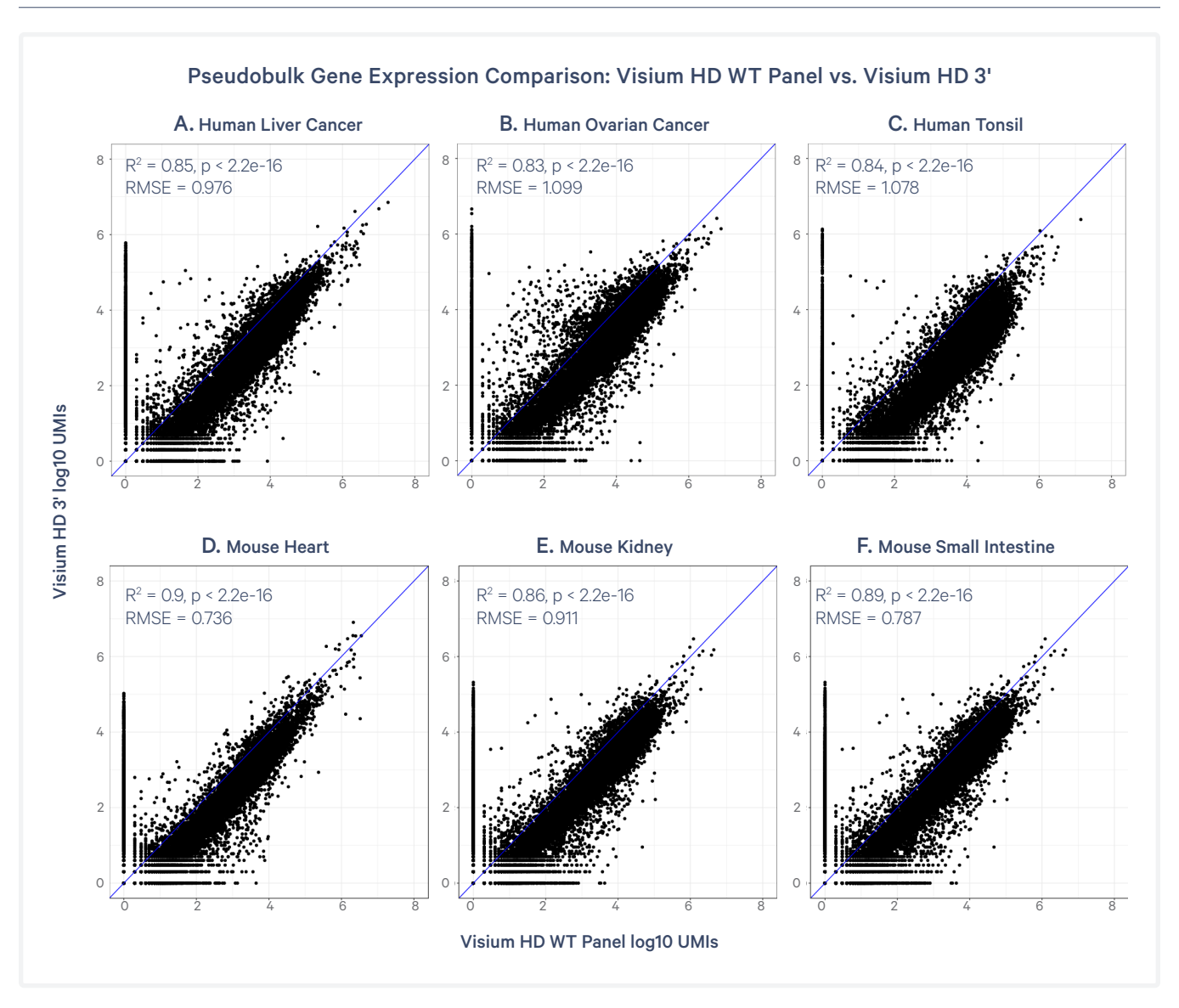


Figure 20. Pseudobulk gene expression comparisons for Visium HD WT Panel vs. Visium HD 3' for the following FF samples: human liver cancer (A), human ovarian cancer (B), human tonsil (C), mouse heart (D), mouse kidney (E), and mouse small intestine (F). Pseudobulk analysis samples were downsampled to matched depths using the R function DropletUtils::downsampleReads.

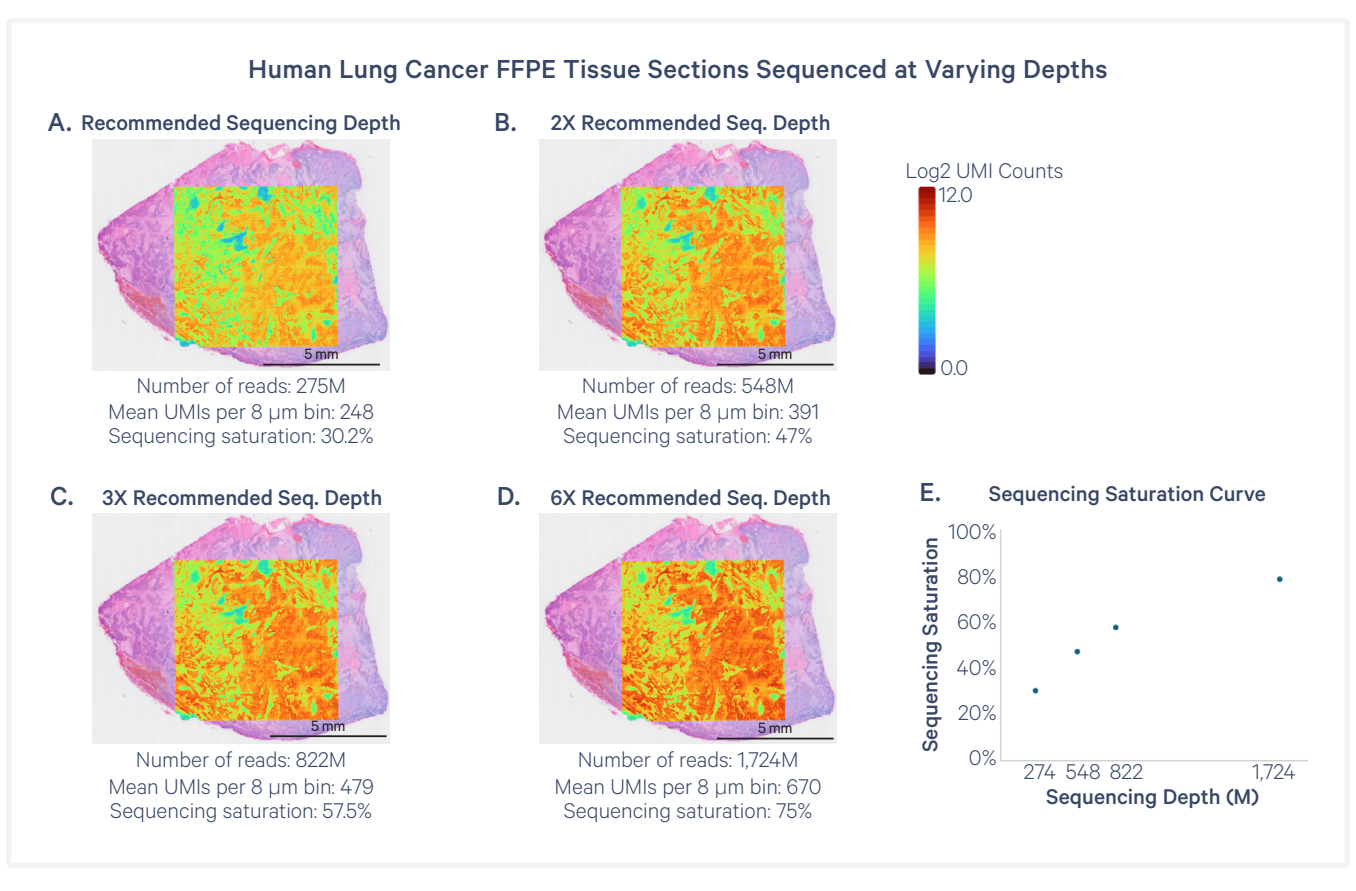


Figure 21. Human lung cancer FFPE samples sequenced at the recommended sequencing depth for Visium HD WT Panel is 275 million read pairs multiplied by the percentage of the Capture Area covered by FFPE tissue (A), 2x the recommended sequencing depth (B), 3x the recommended sequencing depth (C), and 6x the recommended sequencing depth (D). Binned UMI heat maps (log2) are overlaid onto the H&E image in each panel. Mean UMIs per 8 µm bin are 248 for (A), 391 for (B), 479 for (C), and 670 for (D). As sequencing depth increases, saturation increases up to 75% at 6x the recommended sequencing depth (E).

#### **Data Considerations**

### **gDNA**

The Visium HD WT Panel assay results in highresolution, reproducible data with minimal contribution of genomic DNA. UMI counts from gDNA arise from off-target probe ligation events that occur on gDNA strands. Figure 22 summarizes estimated UMI counts from gDNA across a variety of tissues processed with either the Visium HD or Visium v2 assay. The reduction in percentage of reads estimated to come from gDNA is the result of improvements made to the assay for Visium HD, including decreasing the decrosslinking temperature and updating the decrosslinking buffer. For more information on gDNA, consult the Visium CytAssist Spatial Gene Expression for FFPE: Robust Data Analysis with Minimal Impact of Genomic DNA Technical Note (Document CG000605).

### Reproducibility

As shown in Figure 23, Visium HD WT Panel data are reproducible across different lots of Visium HD Slides, supported storage conditions, and supported thermal cyclers. Similarly, the Visium HD 3' assay is reproducible across slides, supported storage conditions, and supported thermal cyclers (data not shown).

#### Visium HD Slide

Due to design and manufacturing complexities of the Visium HD Slides, some artifacts may manifest in Visium HD data that are not seen in Visium v2: however, these differences do not have significant effects on data interpretation. The reasons why these artifacts appear and additional context around data interpretation are discussed below.

When visualizing large numbers of UMIs at once, some rows and columns of bins or 2 µm squares may appear slightly darker or brighter than others. This effect is most apparent when viewing the total UMI map. These "line patterns" appear due to technical variations in the slide manufacturing process that result in a slight variance in the square size and appear as differences in sensitivity when visualized as idealized 2 µm squares. This affects all genes similarly and has minimal impact on spatiality. Since all genes are uniformly affected, secondary analysis such as differential expression or unbiased clustering – which normalize for differences in total UMI count per bin - are minimally impacted. Figure 24 shows the minimal impact of line patterns in areas of high gene expression and the minor impact to unbiased clustering in regions with very low UMI counts. In sample types where there is very little spatial variability in total UMI counts per bin, the variability from line patterns will be more visibly apparent, even though the absolute size of the effect is unchanged. Lines can also appear outside of tissue when UMIs are present in those regions.

To illustrate the minimal impact of line patterns on unbiased clustering, the top differentially expressed genes between the dark blue and yellow clusters in the human lung sample were examined, as these form a line pattern (Figure 25). The most highly expressed genes in the dark blue cluster are also highly expressed in the cyan cluster, indicating that the dark blue cluster is composed of bins bridging the cells marked by cyan and the low transcript density yellow cluster. Additionally, there are very few genes that uniquely identify the yellow cluster, which is an area of low expression. There are no genes that distinguish the dark blue and yellow clusters in any meaningful way; thus, the appearance of the line between the clusters is considered inconsequential.

Visium HD Slides undergo a rigorous manufacturing process that ensures that >99% of the Capture Area is covered with spatiallybarcoded capture oligos; however, localized low UMI recovery can occur as a result of

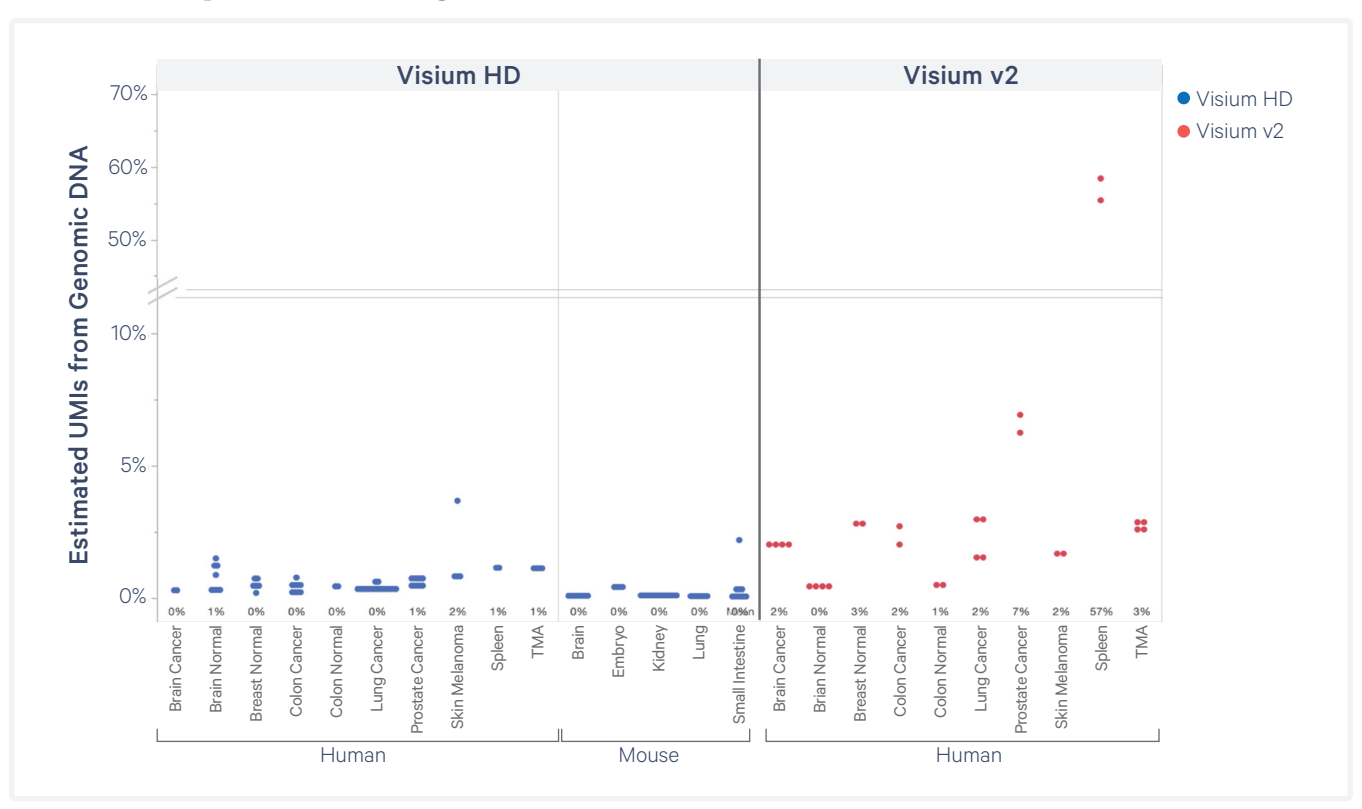


**Figure 22.** Estimated UMI counts from gDNA across various tissues. Mouse data from Visium v2 is not displayed because the Visium v2 assay uses v1 of the mouse probe set, which does not have the required gDNA probes for detection.

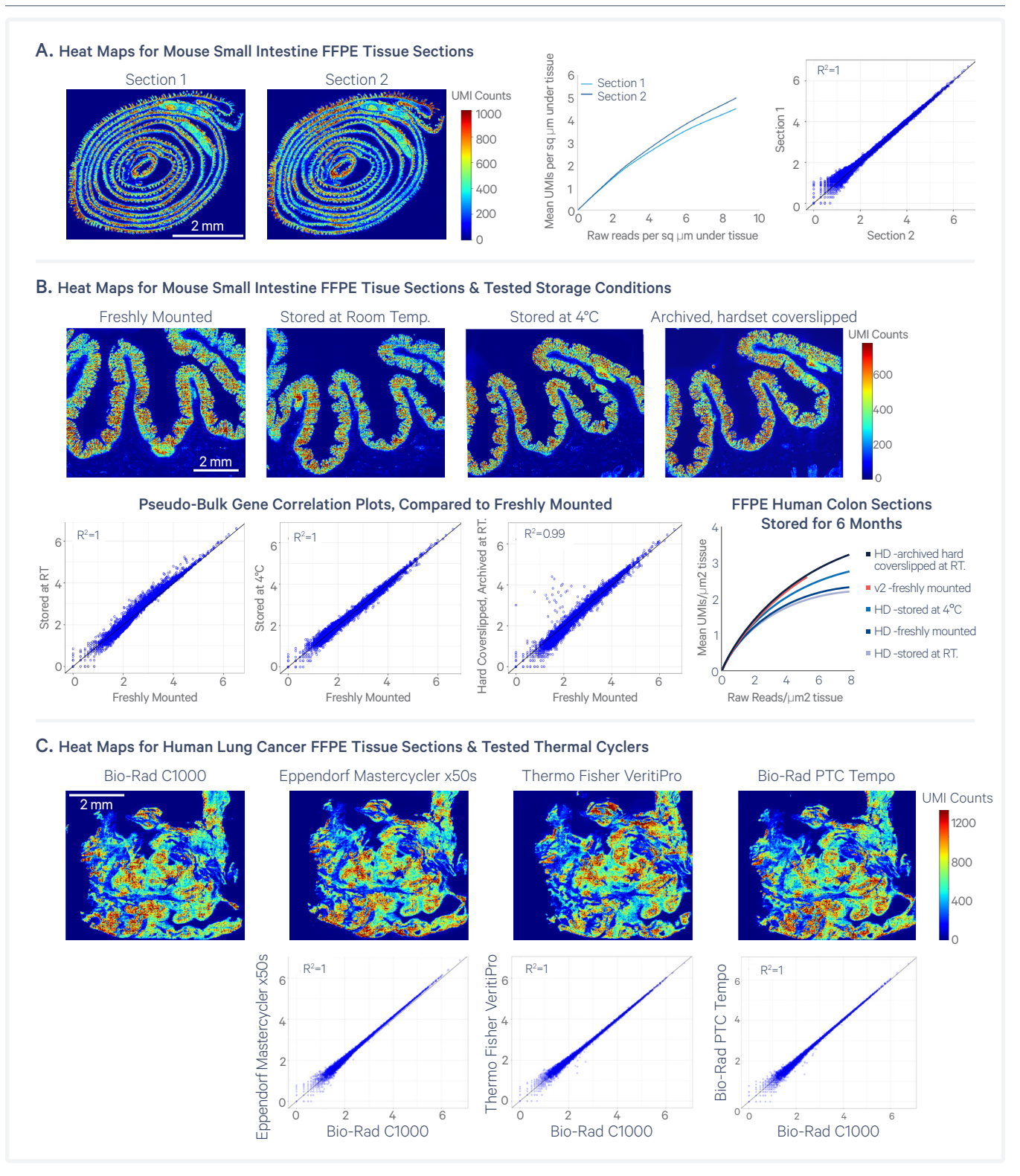


Figure 23. Visium HD WT Panel Assay reproducibility across slide lots, storage conditions, and thermal cyclers. (A) Two sections from the same mouse small intestine FFPE block have similar UMI counts, mean UMIs per square µm under tissue, and have strongly correlated gene expression profiles across slide lots. (B) Human colon FFPE tissue was processed under the indicated conditions. Unless otherwise noted, samples were not coverslipped. At 6 months, archived sections were processed using a freshly-sectioned/ mounted tissue from the same block as control on different CytAssist instruments. UMI heat maps and pseudobulk gene correlation plots between replicates show high correlation. (C) Consecutive sections from a human lung cancer FFPE tissue block were used to test the indicated thermal cyclers. Each condition was run on a different CytAssist instrument. Replicates have consistent UMI heat maps as well as high gene expression correlation between the tested thermal cyclers.

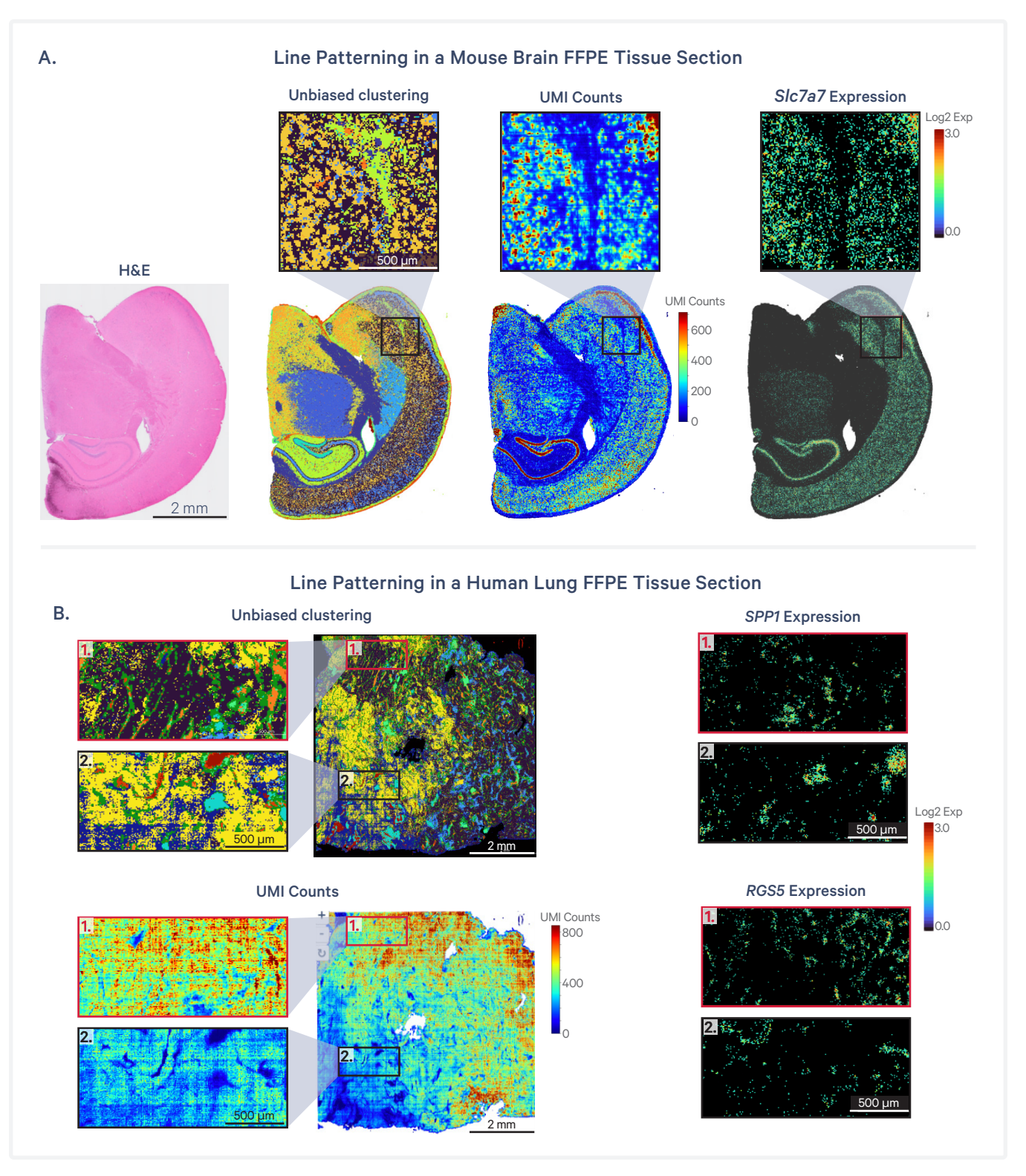
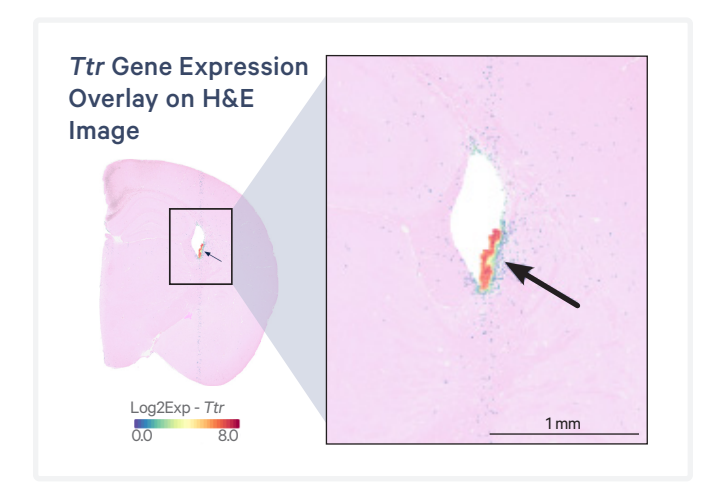


Figure 24. (A) A mouse brain FFPE tissue section that shows a line pattern when viewing unbiased clustering and total UMIs within the area marked with a black box. This line pattern has a negligible impact on the unbiased clustering or the expected localization of key marker genes, such as SIc7a7. (B) A human lung section, where line patterns are more apparent in areas of low expression than in areas of high expression as shown when viewing unbiased clustering or total UMI counts. As with the mouse brain FFPE tissue section, this line patterning has a negligible effect on the expected localization of key marker genes such as SPP1 or RGS5.

manufacturing defects within the Capture Area that result in missing oligos on the slide surface. Additionally, debris on the Visium HD Slide or tissue slide or the presence of bubbles between the tissue and Capture Area may also result in low UMI recovery, as these may inhibit molecules from being captured on the Visium HD Slide and assigned a UMI and Spatial Barcode. To assess the percentage of Spatial Barcodes that match the whitelist, a valid barcode rate is reported in the web summary produced by Space Ranger. This rate is typically above 85% for the Visium HD WT Panel assay and above 75% for the Visium HD 3' assay.

There is a small chance (<1.5%) that errors in the Spatial Barcode oligo sequence result in the assignment of that barcode's sequence to an unexpected location (> 10  $\mu$ m away). This will result in up to 1.5% of all transcripts being improperly located across the tissue. While this has minimal impact on clustering results, it creates low level noise in the data as well as a visual impact to individual gene localization analysis (Figure 26).

While this is only noticeable for highly abundant genes, this mislocalization can occur for any transcript regardless of expression level.



**Figure 26.** A mouse brain FFPE sample demonstrating mislocalization on the highly expressing and highly concentrated Ttr gene. Ttr is expected to only be expressed within the choroid plexus; however, mislocalization of Ttr signal is seen in both the X and Y axes.

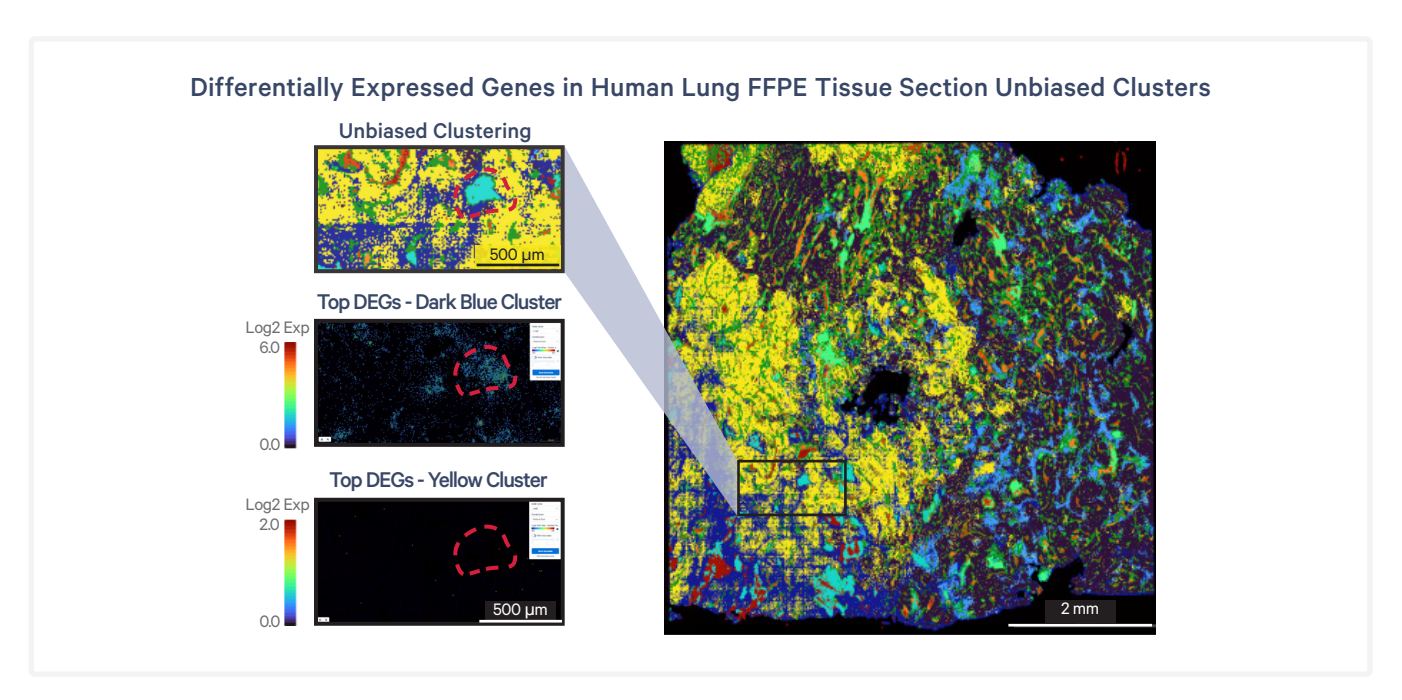


**Figure 25.** Examining the top differentially expressed genes (DEGs) between the yellow and dark blue clusters that form a line pattern in a human lung FFPE sample.

# **Conclusion**

### Conclusion

Visium HD assays enable single cell-scale analysis of gene expression data. This Technical Note described the design of the Visium HD Slide, as well as the data binning strategy Space Ranger utilizes to optimize data interpretation. The data presented in this Technical Note shows that:

- Visium HD and Visium HD 3' retain high spatial resolution through optimal transcript localization and feature dimension that allow whole transcriptome gene expression data to be mapped clearly to relevant biological structures
- Sensitivity comparisons are tissue-dependent,
  - Visium HD WT Panel typically has comparable sensitivity to Visium v2
  - Visium HD 3' has improved sensitivity vs. Visium v1
  - Visium HD WT Panel for fresh frozen tissues has higher sensitivity compared to Visium HD 3'
- · Visium HD assays are reproducible across different lots of Visium HD Slides, CytAssist instruments, serial tissue sections, and thermal cyclers
- · Visium HD WT Panel Assay optimizes data quality and minimizes the percentage of reads estimated to come from gDNA

### References

- Visium CytAssist Tissue Preparation Guide (CG000518)
- Visium CytAssist H&E Staining Demonstrated Protocol (CG000520)
- Visium CytAssist Spatial Gene Expression Reagent Kits User Guide (CG000495)
- Visium HD FFPE Tissue Preparation Handbook (CG000698)
- · Visium HD FF Tissue Preparation Handbook (CG000763)
- Visium HD 3' FF Tissue Preparation Handbook (CG000804)
- Visium HD Spatial Applications Imaging Guidelines (CG000688)
- · Visium HD Spatial Gene Expression Reagent Kits User Guide (CG000685)
- Visium HD 3' Spatial Gene Expression Reagent Kits User Guide (CG000805)
- Visium CytAssist Spatial Gene Expression for FFPE: Robust Data Analysis with Minimal Impact of Genomic DNA (CG000605)

# **Appendix**

## **Workflow Comparisons**

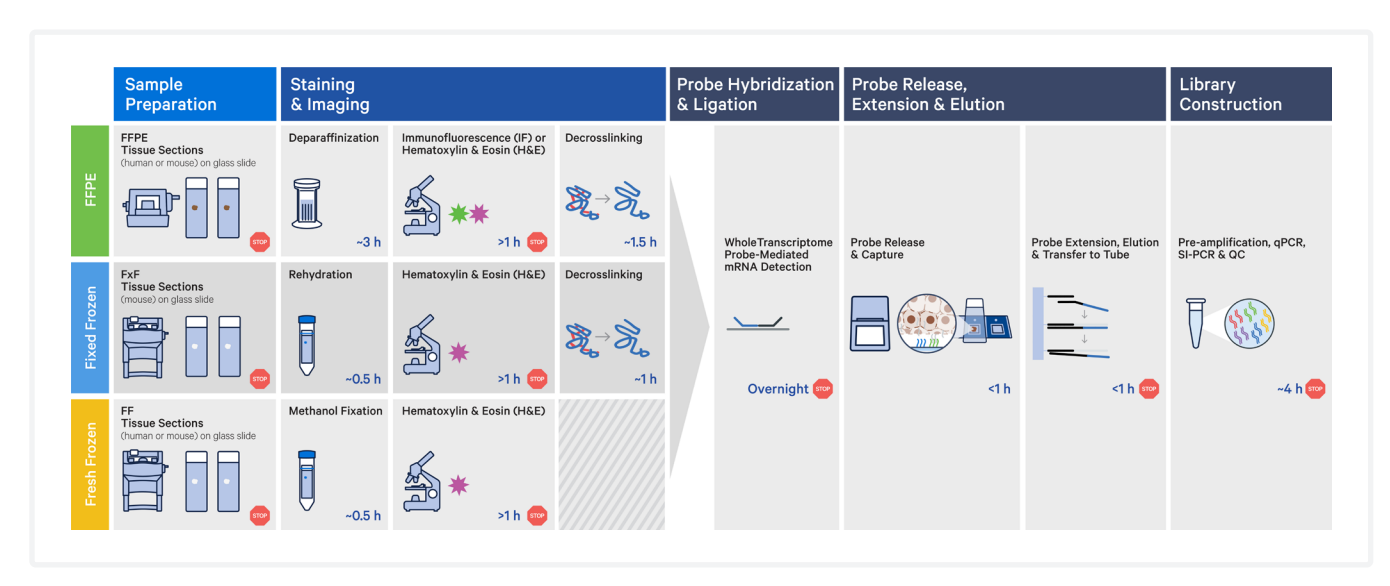


Figure A1. Workflow overview for Visium v2 Spatial Gene Expression.



Figure A2. Workflow overview for Visium HD WT Panel Spatial Gene Expression.

### **Document Revision Summary**

**Document Number** CG000686

Title Visium HD Spatial Applications Performance Technical Note

Revision Rev B

**Revision Date** September 2024

- Renamed Technical Note to Visium HD Spatial Applications Performance to be inclusive of all Visium HD assays.
- Added key terminology for assays on cover page.
- Added table of contents to page 2.
- Added workflow comparison of Visium HD 3' and Visium v1 to page 3.
- Added description of Visium HD 3' Spatial Gene Expression assay to page 3.
- Added size comparison of Visium v1 and Visium HD Slides with Visium HD 3' data to page 5.
- Added information on barcode and UMI region on Visium HD Slide to page 6.
- Added information on Visium HD 3' Gene Expression methods to page 7.
- Added information on cell segmentation to page 9.
- Added Visium HD 3' data highlights to page 14–16.
- Added information on Visium HD 3' assay sensitivity to pages 17–20
- Corrected recommended sequencing depth in figure 21 on page 21.
- Added conclusion on Visium HD 3' to page 27.
- Added Visium HD 3' FF Tissue Preparation Handbook and Visium HD 3' Spatial Gene Expression Reagent Kits User Guide to page 27.
- Added workflow overviews for Visium v2 and Visium HD WT Panel to page 28.
- · Changed references to "Visium HD" to "Visium HD WT Panel" throughout for clarity.

© 2025 10x Genomics, Inc. (10x Genomics). All rights reserved. Duplication and/or reproduction of all or any portion of this document without the express written consent of 10x Genomics, is strictly forbidden. Nothing contained herein shall constitute any warranty, express or implied, as to the performance of any products described herein. Any and all warranties applicable to any products are set forth in the applicable terms and conditions of sale accompanying the purchase of such product. 10x Genomics provides no warranty and hereby disclaims any and all warranties as to the use of any third-party products or protocols described herein. The use of products described herein is subject to certain restrictions as set forth in the applicable terms and conditions of sale accompanying the purchase of such product. A non-exhaustive list of 10x Genomics' marks, many of which are registered in the United States and other countries can be viewed at: www.10xgenomics.com/trademarks. 10x Genomics may refer to the products or services offered by other companies by their brand name or company name solely for clarity, and does not claim any rights in those third-party marks or names. 10x Genomics products may be covered by one or more of the patents as indicated at: www.10xgenomics.com/patents. All products and services described herein are intended FOR RESEARCH USE ONLY and NOT FOR USE IN DIAGNOSTIC PROCEDURES.

The use of 10x Genomics products in practicing the methods set forth herein has not been validated by 10x Genomics, and such non-validated use is NOT COVERED BY 10X GENOMICS STANDARD WARRANTY, AND 10X GENOMICS HEREBY DISCLAIMS ANY AND ALL WARRANTIES FOR SUCH USE. Nothing in this document should be construed as altering, waiving or amending in any manner 10x Genomics terms and conditions of sale for the Chromium Controller or the Chromium Single Cell Controller, consumables or software, including without limitation such terms and conditions relating to certain use restrictions, limited license, warranty and limitation of liability, and nothing in this document shall be deemed to be Documentation, as that term is set forth in such terms and conditions of sale. Nothing in this document shall be construed as any representation by 10x Genomics that it currently or will at any time in the future offer or in any way support any application set forth herein.

#### **Contact:**

support@10xgenomics.com

10x Genomics, Inc. 6230 Stoneridge Mall Road Pleasanton, CA 94588 USA

